
Article:
Aad, G. orcid.org/0000-0002-6665-4934, Abbott, B. orcid.org/0000-0002-5888-2734, Abbott, D.C. orcid.org/0000-0002-7248-3203 et al. (2913 more authors) (2023) Search for pair-produced vector-like top and bottom partners in events with large missing transverse momentum in pp collisions with the ATLAS detector. The European Physical Journal C, 83. 719.

https://doi.org/10.1140/epjc/s10052-023-11790-7

Eur. Phys. J. C (2023) 83:719
https://doi.org/10.1140/epjc/s10052-023-11790-7

THE EUROPEAN PHYSICAL JOURNAL C

Regular Article - Experimental Physics

Search for pair-produced vector-like top and bottom partners in events with large missing transverse momentum in pp collisions with the ATLAS detector

ATLAS Collaboration[*]

CERN, 1211 Geneva 23, Switzerland

Received: 13 December 2022 / Accepted: 2 July 2023

Abstract A search for pair-produced vector-like quarks using events with exactly one lepton (e or μ), at least four jets including at least one b-tagged jet, and large missing transverse momentum is presented. Data from proton–proton collisions at a centre-of-mass energy of $\sqrt{s}$ =13 TeV, recorded by the ATLAS detector at the LHC from 2015 to 2018 and corresponding to an integrated luminosity of 139 fb^{-1}, are analysed. Vector-like partners T and B of the top and bottom quarks are considered, as is a vector-like X with charge +5/3, assuming their decay into a W, Z, or Higgs boson and a third-generation quark. No significant deviations from the Standard Model expectation are observed. Upper limits on the production cross-section of T and B quark pairs as a function of their mass are derived for various decay branching ratio scenarios. The strongest lower limits on the masses are 1.59 TeV assuming mass-degenerate vector-like quarks and branching ratios corresponding to the weak-isospin doublet model, and 1.47 TeV (1.46 TeV) for exclusive $T \to Zt$ ($B/X \to Wt$) decays. In addition, lower limits on the T and B quark masses are derived for all possible branching ratios.

Contents

1 Introduction

The fine-tuning or naturalness problem [1] in particle physics arises from loop corrections to the Higgs boson mass that are quadratically divergent. If the Standard Model were complete, those would lead to corrections to the Higgs mass of the order of the Planck scale, 10^{19} GeV, and a finely tuned bare Higgs mass of a similar value is needed to arrive at the measured mass of about 125 GeV [2].

Vector-like quarks (VLQs) [3–6] could dampen the unnaturally large quadratic corrections to the Higgs boson mass by contributing significantly to loop corrections. They are hypothetical spin-1/2 coloured particles whose left-handed and right-handed states have the same electroweak coupling. They appear in a number of theories beyond the Standard Model (SM) of particle physics, mainly in the 'Little Higgs' [7–9] and 'Composite Higgs' [10,11] classes of models.

At the large hadron collider (LHC), VLQs could be produced singly via electroweak interactions or in pairs mainly via the strong interaction. While the cross-section for the latter depends only on the VLQ mass, the former has an additional dependence on the unknown coupling strength between the electroweak bosons and the VLQ. VLQs are expected to preferentially couple to third-generation quarks [3,12]. Therefore the up-type VLQ T with charge +2/3 is in the following assumed to only have the three possible decay modes $T \to Zt$, $T \to Ht$, and $T \to Wb$. Similarly, the down-type VLQ B with charge −1/3 can decay into Zb, Hb, or Wt. Vector-like X quarks with charge +5/3 also appear in multiplets with T partners [4,13] and decay via $X \to Wt$ only.

This analysis investigates all possible decay modes and combinations of branching ratios for the pair-produced vector-like T (VLT) quark and B (VLB) quark, shown in Fig. 1. However, it is most sensitive to the $T \to Zt$ and $B \to Wt$ decays. Since the analysis does not distinguish between particles and antiparticles, the limits for $B \to Wt$

[*] e-mail: atlas.publications@cern.ch

Published online: 10 August 2023

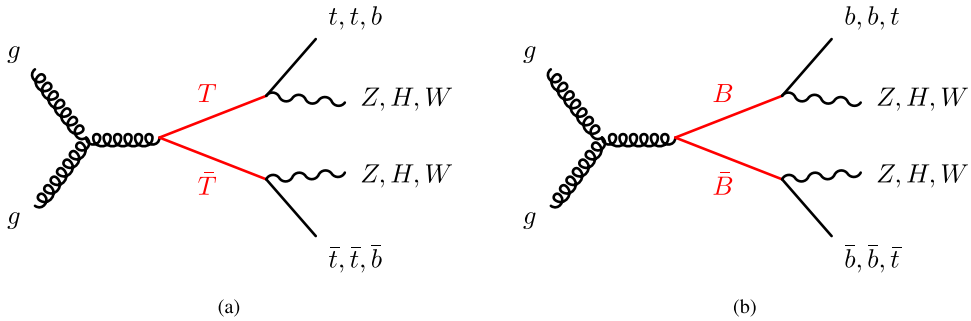

Fig. 1 Representative Feynman diagrams for **a** $T\bar{T}$ and **b** $B\bar{B}$ production and decay. In the analysis, no distinction is made between particles and antiparticles, leading to sensitivity to the $X\bar{X} \to WtWt$ final state as well

also apply to the vector-like X quark, given that it exclusively decays into Wt. Particular combinations of branching ratios correspond to the weak-isospin singlet and doublet models. For T and B quarks, the branching ratio for each decay mode depends on the VLQ mass and weak-isospin quantum numbers [4]. The branching ratios given in the following are for VLQ masses above 800 GeV, where they are approximately independent of the VLQ mass. For a singlet T, all decay modes have sizeable branching ratios ($\mathcal{B}(Zt, Ht, Wb) \approx (0.25, 0.25, 0.5)$), whereas if T is in either an (X, T) doublet or a (T, B) doublet, it decays only into Zt or Ht with equal branching ratios as long as the generalised Cabibbo–Kobayashi–Maskawa (CKM) matrix elements fulfil $|V_{Tb}| \ll |V_{Bt}|$ [4]. Similarly, for a singlet B the branching ratios of all decay modes are sizeable ($\mathcal{B}(Zb, Hb, Wt) \approx (0.25, 0.25, 0.5)$), while for the (T, B) doublet scenario with $|V_{Tb}| \ll |V_{Bt}|$ the $B \to Wt$ decay is the only possibility.

The results are based on the full Run 2 (2015–2018) dataset collected by the ATLAS experiment in $\sqrt{s}$ =13 TeV proton–proton collisions at the LHC, corresponding to an integrated luminosity of 139 fb^{-1}. Several searches for pair-produced VLQs targeting various final states have already been performed by ATLAS [14–21] and CMS [22–25]. Those results are based on a subset of the Run 2 data of about 36 fb^{-1}, except for Refs. [21,25]. A combination of the ATLAS results using the 36 fb^{-1} dataset is also available [26], excluding T (B) masses below 1.31 TeV (1.03 TeV) for any combination of the three decay modes per VLQ discussed above.

The analysis is based on a final-state signature with high missing transverse momentum $E_{\mathrm{T}}^{\mathrm{miss}}$, one lepton ℓ (e or μ), and at least four jets including a b-tagged jet. The previous ATLAS search in this final state is based on a subset of the Run 2 data [16], yielding lower limits on the T quark mass of 1.16 TeV for $\mathcal{B}(T \to Zt) = 100\%$ and 0.87 TeV (1.05 TeV) for the T in the singlet (doublet) model. Here the analysis is extended mainly by also investigating vector-like B quarks and by using neural networks (NNs) trained at several branching ratios in order to separate signal from background, instead of using a cut-and-count analysis with a single signal region (SR). The training is done separately for T and B in a common training region using simulated events. The SRs are each defined by a subset of the training region passing a selection on the corresponding NN output. Control regions (CRs) are defined so as to be enriched in the various background processes. They are orthogonal to the training region, and thus to the SRs, and orthogonal to each other. The statistical interpretation is based on a simultaneous fit to the CRs and SR for T or B, in which the normalisations for $t\bar{t}$, W+jets and single-top-quark backgrounds and a possible signal contribution are determined.

2 ATLAS detector

The ATLAS experiment [27] at the LHC is a multipurpose particle detector with a forward–backward symmetric cylindrical geometry and a near 4π coverage in solid angle.[1] It consists of an inner tracking detector (ID) surrounded by a thin superconducting solenoid providing a 2T axial magnetic field, electromagnetic and hadron calorimeters, and a muon spectrometer. The inner tracking detector covers the pseudorapidity range $|\eta| < 2.5$. It consists of silicon pixel, silicon microstrip, and transition radiation tracking detectors. Lead/liquid-argon (LAr) sampling calorimeters provide electromagnetic (EM) energy measurements with high granularity. A steel/scintillator-tile hadron calorimeter covers the central pseudorapidity range ($|\eta| < 1.7$). The endcap and forward regions are instrumented with LAr calorimeters for both the EM and hadronic energy measurements up to $|\eta| = 4.9$. The muon spectrometer surrounds the calorimeters and is based on three large superconducting air-core toroidal magnets with eight coils each. The field integral of the toroids ranges between 2.0 and 6.0 T m across most of the detector. The muon spectrometer includes a system of precision tracking chambers and fast detectors for triggering. A two-

[1] ATLAS uses a right-handed coordinate system with its origin at the nominal interaction point (IP) in the centre of the detector and the z-axis along the beam pipe. The x-axis points from the IP to the centre of the LHC ring, and the y-axis points upwards. Cylindrical coordinates (r, ϕ) are used in the transverse plane, ϕ being the azimuthal angle around the z-axis. The pseudorapidity is defined in terms of the polar angle θ as $\eta = -\ln\tan(\theta/2)$. Angular distance is measured in units of $\Delta R \equiv \sqrt{(\Delta\eta)^2 + (\Delta\phi)^2}$.

Table 1 List of ME generator, PDF set, PS model, and tune for the signal and different background processes

Process	ME generator	PDF set	PS and hadronisation	Tune
VLQ signal	PROTOS v2.2	NNPDF 2.3LO	PYTHIA 8.186	A14
$t\bar{t}$/single top	POWHEG BOX v2	NNPDF 3.0NLO	PYTHIA 8.230/8.235	A14
V+jets	SHERPA 2.2.1	NNPDF 3.0NNLO	SHERPA	Internal
Diboson	SHERPA 2.2.1–2.2.2	NNPDF 3.0NNLO	SHERPA	Internal
$t\bar{t}V$	MADGRAPH5_AMC@NLO 2.3.3	NNPDF 3.0NLO	PYTHIA 8.210	A14
$tWZ(\to \nu\nu)$	MADGRAPH5_AMC@NLO 2.6.7	NNPDF 3.0NLO	PYTHIA 8.244	A14
$t\bar{t}H$	POWHEG BOX v2	NNPDF 3.0NLO	PYTHIA 8.230	A14

level trigger system is used to select events. The first-level trigger is implemented in hardware and uses a subset of the detector information to accept events at a rate below 100 kHz. This is followed by a software-based high-level trigger (HLT) that reduces the accepted event rate to 1 kHz on average depending on the data-taking conditions. An extensive software suite [28] is used in data simulation, in the reconstruction and analysis of real and simulated data, in detector operations, and in the trigger and data acquisition systems of the experiment.

3 Data and simulated event samples

The analysis uses data from proton–proton (pp) collisions at $\sqrt{s} = 13$ TeV recorded with the ATLAS detector at the LHC in the years 2015 to 2018. The dataset, collected during stable beam conditions and with all detector subsystems operational [29], corresponds to an integrated luminosity of 139 fb^{-1} with an uncertainty of 1.7% [30]. At the high luminosities reached at the LHC, events are affected by additional inelastic pp collisions in the same or neighbouring bunch crossings, referred to as pile-up. The average number of interactions per bunch crossing was 33.7. Events were selected online during data-taking by $E_{\mathrm{T}}^{\mathrm{miss}}$ triggers [31] with an $E_{\mathrm{T}}^{\mathrm{miss}}$ threshold of 70 GeV in the HLT in 2015 and a threshold rising from 90 GeV to 110 GeV during the later years.

Monte Carlo (MC) simulated events are used for the modelling of the background processes and the VLQ signals. Details of the simulated nominal samples, including the matrix-element (ME) generator and the parton distribution function (PDF) set, the parton shower (PS) and hadronisation model, and the set of tuned parameters (tune), are summarised in Table 1.

The generated events were processed through a simulation [32] of the ATLAS detector geometry and response using GEANT4 [33]. A faster simulation, which employed a parameterisation of the calorimeter response, was used in some cases to estimate systematic uncertainties. In these cases, the systematically varied samples were compared with versions of the nominal samples that were also processed through the fast simulation. In order to model pile-up effects, minimum-bias pp interactions were generated with PYTHIA 8.186 [34] using the A3 [35] set of tuned parameters and overlaid on the simulated hard-scatter events. The resulting events were weighted to match the pile-up profile of the recorded data.

Finally, the simulated events were reconstructed using the same software as the collision data. Corrections were applied to the simulated events in order to match object identification efficiencies, energy scales and resolution to those determined from data in auxiliary measurements.

Signal samples for the pair-production of vector-like T and B quarks were generated at leading order (LO) with PROTOS v2.2 [36] using the NNPDF 2.3LO PDF [37] set, interfaced with PYTHIA 8.186 to model the parton shower, hadronisation, and underlying event. Using the narrow-width approximation, the samples were produced for masses from 800 GeV up to 2 TeV, with a mass spacing of 100 GeV from 1 to 1.8 TeV. The chirality-dependent couplings of the VLQs were set to those in the weak-isospin singlet model, but with equal branching ratios into the three decay modes (Zt, Ht, Wb) for the vector-like T quark and (Zb, Hb, Wt) for the vector-like B quark. Dedicated signal samples in the doublet model were produced for the 1.2 TeV mass point in order to test for potential kinematic biases from the assumed singlet couplings. For the T quark, this choice is conservative because the acceptance is higher in the doublet case, while for the B quark the acceptances are similar for singlet and doublet couplings. In order to obtain the desired branching ratios, an event-by-event reweighting based on generator information is performed. The signal sample cross-sections were calculated with TOP++ 2.0 [38] at next-to-next-to-leading order (NNLO) in QCD including the resummation of next-to-next-to-leading logarithmic (NNLL) soft-gluon terms.

The production of $t\bar{t}$ events was modelled using the POWHEG BOX v2 [39–42] generator at next-to-leading order (NLO) with the NNPDF 3.0NLO set [43] of PDFs and the h_{damp} parameter[2] set to $1.5\,m_t$ [44], with $m_t = 172.5$ GeV.

[2] The h_{damp} parameter is a resummation damping factor and one of the parameters that controls the matching of POWHEG matrix elements to the PS and thus regulates the high-p_{T} radiation against which the $t\bar{t}$ system recoils.

The events were interfaced to PYTHIA 8.230. The cross-section was corrected to the theory prediction at NNLO including NNLL soft-gluon terms calculated using TOP++ 2.0.

Samples of single-top-quark events were produced with the POWHEG BOX v2 generator at NLO in QCD using the NNPDF 3.0NLO set of PDFs with the five-flavour scheme for tW production and s-channel single-top production, and the four-flavour scheme for t-channel single-top events. The tW sample was modelled using the diagram removal scheme [45] to remove interference and overlap with $t\bar{t}$ production. The events were interfaced with either PYTHIA 8.230 or PYTHIA 8.235. The samples were normalised to their NLO QCD cross-sections [46,47], with additional NNLL soft-gluon terms for tW production [48,49].

The production of V+jets ($V = W, Z$) was simulated with the SHERPA 2.2.1 generator using NLO-accurate matrix elements for up to two partons, and LO matrix elements for up to four partons, calculated with the Comix [50] and OPENLOOPS [51–53] libraries. They were matched with the SHERPA PS [54] using the MEPS@NLO prescription [55–58] and the set of tuned parameters developed by the SHERPA authors. The NNPDF 3.0NNLO set of PDFs was used and the samples were normalised to a NNLO prediction [59].

Samples of diboson final states (VV) were simulated with the SHERPA 2.2.1 or 2.2.2 generator, depending on the process, including off-shell effects and Higgs boson contributions where appropriate. Fully leptonic final states and semileptonic final states, where one boson decays leptonically and the other one hadronically, were generated using matrix elements at NLO accuracy in QCD for up to one additional parton and at LO accuracy for up to three additional parton emissions. The matching of NLO matrix elements to the PS and the merging of different jet multiplicities was done in the same way as for V+jets production. The NNPDF 3.0NNLO set of PDFs was used, along with the SHERPA-internal tune. The diboson event samples were normalised to the total cross-section calculated by SHERPA at NLO in QCD.

The production of $t\bar{t}W$ and $t\bar{t}Z$ events was modelled using the MADGRAPH5_AMC@NLO 2.3.3 [60] generator at NLO with the NNPDF 3.0NLO PDF set. The events were interfaced to PYTHIA 8.210. Similarly, the production of tWZ events was modelled using MADGRAPH5_AMC@NLO 2.6.8 at NLO with the NNPDF 3.0NLO PDF set, interfaced to PYTHIA 8.244. The diagram removal scheme was employed to handle the interference between tWZ and $t\bar{t}Z$, and was applied to the tWZ sample. Samples for the production of $t\bar{t}H$ events were generated using the POWHEG BOX v2 generator at NLO with the NNPDF 3.0NLO PDF set, interfaced to PYTHIA 8.230. The generated samples for $t\bar{t}W$, $t\bar{t}Z$, tWZ, and $t\bar{t}H$ production were normalised to NLO cross-section predictions calculated by MADGRAPH5_AMC@NLO.

All simulated samples, except those produced with the SHERPA [61] event generator, utilised the EVTGEN [62] program to model the decay of heavy-flavour hadrons. While EVTGEN 1.2.0 was used for the VLQ signal samples and the $t\bar{t}V$ samples, EVTGEN 1.6.0 was used in all other cases. For all nominal samples where PYTHIA 8 [63] was utilised for the showering and hadronisation, PYTHIA was used with the A14 [64] set of tuned parameters and the NNPDF 2.3LO set of PDFs.

4 Event reconstruction and object selection

Events are required to have at least one pp collision vertex candidate with at least two associated tracks with transverse momentum $p_{\mathrm{T}} > 0.5$ GeV. The primary vertex is defined to be the vertex candidate with the largest scalar sum of transverse momenta of all associated tracks. In this analysis, electrons, muons, and jets are the calibrated physics objects used. For the charged leptons, two sets of quality and kinematic requirements are imposed, where the selection for signal leptons is tighter than for baseline leptons.

Electron candidates are reconstructed from energy deposits in the EM calorimeter matched to charged-particle tracks in the ID. Baseline electrons are required to have $p_{\mathrm{T}} > 10$ GeV and to be reconstructed within $|\eta| < 2.47$, excluding the barrel–endcap transition region $1.37 < |\eta| < 1.52$. They must fulfil 'loose' identification criteria, using a likelihood-based discriminant that combines information about tracks in the ID and energy deposits in the calorimeter system [65], and are required to have a hit in the innermost layer of the pixel detector. Furthermore, isolation requirements in both the calorimeter and the ID are imposed [65]. An electron does not meet the isolation criteria if, after subtracting contributions from pile-up and the electron itself, the transverse energy deposited in the calorimeter within a surrounding cone of radius $\Delta R = 0.2$ exceeds 20% of the transverse energy of the electron. Similarly, electron candidates are excluded if the scalar sum of the transverse momenta of tracks within a cone of radius $\Delta R = \min(10\,\mathrm{GeV}/p_{\mathrm{T}}(e), 0.2)$, excluding the track matched to the electron, is larger than 15% of the electron p_{T}. In addition, each electron candidate's track must be matched to the primary vertex. This requires that the significance of its transverse impact parameter, d_0, satisfies $|d_0|/\sigma_{d_0} < 5$, where σ_{d_0} is the uncertainty in d_0, and that the longitudinal distance z_0 from the primary vertex to the point where d_0 is measured satisfies $|z_0 \sin\theta| < 0.5$mm. In order to suppress backgrounds due to hadrons misidentified as electrons, signal electrons must satisfy all baseline criteria and in addition 'tight' identification criteria [65], and have $p_{\mathrm{T}} > 28$ GeV.

Muon candidates are reconstructed by combining charged-particle tracks formed in the ID and in the muon spectrometer

or by matching ID tracks to an energy deposit in the calorimeter compatible with a minimum ionising particle [66]. Baseline muons are required to have $p_{\mathrm{T}} > 10\,\mathrm{GeV}$ and $|\eta| < 2.5$, and to satisfy the 'loose' identification criteria [66]. Track-to-vertex matching is ensured by requiring the muon track to satisfy $|d_0|/\sigma_{d_0} < 3$ and $|z_0 \sin\theta| < 0.5\mathrm{mm}$. Signal muons must satisfy 'medium' identification criteria and are required to have $p_{\mathrm{T}} > 28\,\mathrm{GeV}$. Additionally, signal muons must be isolated, requiring that the scalar p_{T} sum of all tracks within a cone of radius $\Delta R = \min(10\,\mathrm{GeV}/p_{\mathrm{T}}(\mu), 0.3)$ around the muon is less than 6% of the muon p_{T}.

Small-radius (small-R) jet candidates are built from particle-flow objects [67,68], using the anti-k_t algorithm [69,70] with a radius parameter of $R = 0.4$. The particle-flow algorithm combines information about tracks in the ID and energy deposits in the calorimeters to form the input for the jet reconstruction. Jets are required to have $p_{\mathrm{T}} > 25\,\mathrm{GeV}$ and $|\eta| < 2.5$. To reject jets originating from pile-up interactions, jet candidates with $|\eta| < 2.4$ and $p_{\mathrm{T}} < 60\,\mathrm{GeV}$ are required to satisfy the 'tight' jet vertex tagger (JVT) criterion [71]. Small-R jets containing a b-hadron decay are b-tagged using a multivariate algorithm, called DL1r, operating at a tagging efficiency of 77% as determined in simulated $t\bar{t}$ events [72,73].

An overlap removal procedure is applied to prevent double counting of ambiguous reconstructed objects, using the baseline lepton definitions. First, electron–muon overlap is handled by removing muons sharing a track in the ID with an electron if the muon is calorimeter-tagged, and otherwise removing the electron. Subsequently, overlap between jets and leptons is removed by rejecting any jets within $\Delta R = 0.2$ of an electron and afterwards rejecting any electrons within $\Delta R = 0.4$ of a jet. Similarly, jets are discarded if they have fewer than three associated tracks and are within $\Delta R = 0.2$ of a muon candidate. Otherwise, the muon is rejected if it lies within $\Delta R = \min(0.4, 0.04 + 10\,\mathrm{GeV}/p_{\mathrm{T}}(\mu))$ of a jet.

The missing transverse momentum, with magnitude $E_{\mathrm{T}}^{\mathrm{miss}}$, is defined as the negative vectorial sum of the transverse momenta of all calibrated objects in an event, plus a track-based soft-term which takes into account energy depositions associated with the primary vertex but not with any calibrated object [74].

Finally, large-radius (large-R) jets are constructed from the selected small-R jets using the anti-k_t algorithm with $R = 1.0$. In order to reduce the impact of soft radiation, constituent small-R jets with p_{T} less than 5% of the large-R jet p_{T} are removed. These reclustered large-R jets are required to have $p_{\mathrm{T}} > 150\,\mathrm{GeV}$ and a mass larger than 50 GeV.

5 Event selection and categorisation

All events considered in this analysis must be selected by an $E_{\mathrm{T}}^{\mathrm{miss}}$ trigger. Since the trigger thresholds were raised during Run 2, a requirement of $E_{\mathrm{T}}^{\mathrm{miss}} > 250\,\mathrm{GeV}$ is imposed to ensure full trigger efficiency over all data-taking periods. Events are also required to have exactly one signal lepton (e, μ) and at least four small-R jets of which at least one is b-tagged. A veto on a second lepton, fulfilling the baseline requirements, is used to suppress $t\bar{t}$ events with two leptons in the final state. To reject events with $E_{\mathrm{T}}^{\mathrm{miss}}$ arising from mismeasured jets, the azimuthal angle between the missing transverse momentum vector $\vec{E}_{\mathrm{T}}^{\mathrm{miss}}$ and both the leading (j_1) and subleading (j_2) jets, ordered in p_{T}, must satisfy the condition $|\Delta\phi(j_i, \vec{E}_{\mathrm{T}}^{\mathrm{miss}})| > 0.4$, with $i \in \{1, 2\}$. In addition, events must have a transverse mass $m_{\mathrm{T}}^{W} > 30\,\mathrm{GeV}$, where m_{T}^{W} is defined as

$$m_{\mathrm{T}}^{W} = \sqrt{2 p_{\mathrm{T}}(\ell) E_{\mathrm{T}}^{\mathrm{miss}} \left[1 - \cos\left(\Delta\phi(\ell, \vec{E}_{\mathrm{T}}^{\mathrm{miss}})\right)\right]}.$$

After applying these requirements, referred to as 'preselection' in Table 2, the dominant backgrounds come from $t\bar{t}$ and W+jets production. A training region for the NNs is defined by applying further requirements listed in Table 2, which reduce the amount of background without decreasing the sensitivity to the signal. Requiring m_{T}^{W} to be well above the W boson mass peak, $m_{\mathrm{T}}^{W} > 120\,\mathrm{GeV}$, strongly reduces the W+jets and semileptonic $t\bar{t}$ background. In these background processes the leptonic W boson decay is the only source of $E_{\mathrm{T}}^{\mathrm{miss}}$, while in the VLQ pair production additional sources of $E_{\mathrm{T}}^{\mathrm{miss}}$ can arise from e.g., the Z boson decay to neutrinos or the W boson decay to a hadronically-decaying tau-lepton and a neutrino. The remaining $t\bar{t}$ background originates from dileptonic $t\bar{t}$ events where one lepton is not detected. This type of $t\bar{t}$ background is suppressed by requirements on the asymmetric transverse mass, am_{T2} [75,76], which is a variant of the m_{T2} [77,78] variable. The latter is applied to signatures where two or more particles are not detected directly (e.g. dileptonic $t\bar{t}$ events, where the two neutrinos are not detected), and it is defined as

$$m_{\mathrm{T2}} = \min_{\vec{q}_{\mathrm{T}a} + \vec{q}_{\mathrm{T}b} = \vec{E}_{\mathrm{T}}^{\mathrm{miss}}} \left[\max(m_{\mathrm{T}a}, m_{\mathrm{T}b})\right].$$

In this formula, $m_{\mathrm{T}a}$ and $m_{\mathrm{T}b}$ are transverse masses calculated using two sets of one or more visible particles, denoted by a and b, respectively, and all possible combi-

Table 2 Overview of the event selections for the training region that is subdivided into a low-NN_{out} control region and a signal region, for the top reweighting region, and for the control regions for W+jets events and single-top-quark events

Preselection				
$E_{\text{T}}^{\text{miss}}$ triggers				
$= 1$ signal lepton				
no additional baseline lepton				
≥ 4 jets				
≥ 1 b-jet				
$E_{\text{T}}^{\text{miss}} > 250\,\text{GeV}$				
$m_{\text{T}}^{W} > 30\,\text{GeV}$				
$\lvert\Delta\phi(j_{1,2}, \vec{E}_{\text{T}}^{\text{miss}})\rvert > 0.4$				
	Training region low-NN_{out} CR/SR	Top reweighting region	W+jets CR	Single-top CR
m_{T}^{W} [GeV]	> 120	> 120	$\in [30, 120]$	$\in [30, 120]$
am_{T2} [GeV]	> 200	< 180	> 200	> 200
b-jet multiplicity	≥ 1	≥ 1	$= 1$	≥ 2
Large-R jet multiplicity	≥ 1	≥ 1	≤ 1	≤ 1
m(large-R jet) [GeV]	–	–	< 150	< 150
Lepton charge	–	–	$+1$	–
$\Delta R(b_1, b_2)$	–	–	–	> 1.4
NN_{out}	$< 0.5 / \geq 0.5$	–	–	–

nations of missing transverse momenta $\vec{q}_{\text{T}a}$ and $\vec{q}_{\text{T}b}$, with $\vec{q}_{\text{T}a} + \vec{q}_{\text{T}b} = \vec{E}_{\text{T}}^{\text{miss}}$. In the calculation of am_{T2}, the two sets of visible particles are asymmetric as they consist of the one identified signal lepton with one of the two jets with highest b-tagging score on one hand and the other jet on the other. Given the two possible lepton-jet pairings the combination with the lowest am_{T2} is taken. For dileptonic $t\bar{t}$ events, the am_{T2} distribution has a kinematic endpoint at the top-quark mass, while additional sources of $E_{\text{T}}^{\text{miss}}$ extend the distribution towards higher am_{T2} values. Events in the training region have to fulfil $am_{\text{T2}} > 200\,\text{GeV}$. At least one hadronic decay of a high-p_{T} top quark or SM boson is expected for the considered signal. Thus, at least one large-R jet is required in the training region. About 4% of the simulated signal events are reconstructed in the training region for $T\bar{T}$ or $B\bar{B}$ production with pure $T \to Zt$ and $B \to Wt$ decays and a VLQ mass of 1.2 TeV.

The $t\bar{t}$ background, which is a major background in this analysis, is not modelled accurately at high transverse momenta [79,80]. Therefore, a reweighting procedure, referred to as 'top reweighting' in the following, is applied. Reweighting factors are derived in bins of the jet multiplicity (4, 5, 6, $\geq$7) as a function of the effective mass m_{eff}, defined as the scalar sum of the p_{T} of all reconstructed objects and $E_{\text{T}}^{\text{miss}}$. The reweighting factors are determined for the sum of the $t\bar{t}$ and single-top backgrounds using their nominal prediction and are parameterised with a linear function. They are derived from a comparison between data and MC simulation in a dedicated top reweighting region (see Table 2), which is defined in the same way as the training region except for an inverted am_{T2} requirement. This requirement is strengthened to $am_{\text{T2}} < 180\,\text{GeV}$ in order to have a higher $t\bar{t}$ purity of about 90% and less signal contamination in the tails of the m_{eff} distribution. The resulting reweighting factors are applied to $t\bar{t}$ and single-top-quark events in each of the defined analysis regions, which changes the event yields and leads to an improved modelling. This can be seen in Fig. 2 which compares the data with MC simulation in the top reweighting region after reweighting, and also shows the MC expectation before reweighting.

Control regions are defined for the W+jets and single-top-quark backgrounds so as to be enriched in the respective background and have negligible contamination from signal. Both CRs are defined to be orthogonal to the top reweighting region and the training region by modifying the requirement on m_{T}^{W}, using a window of $30\,\text{GeV} < m_{\text{T}}^{W} < 120\,\text{GeV}$ around the W boson mass. In order to reduce the $t\bar{t}$ background contribution in these regions, the large-R jet multiplicity is required to be less than two, and if a large-R jet is present its mass has to be below 150 GeV. For the W+jets CR, the contribution from $t\bar{t}$ events is further reduced by selecting only events with exactly one b-tagged jet. Since the cross-section for W^+ production is larger than for W^- production, higher W+jets purity is achieved by selecting only events

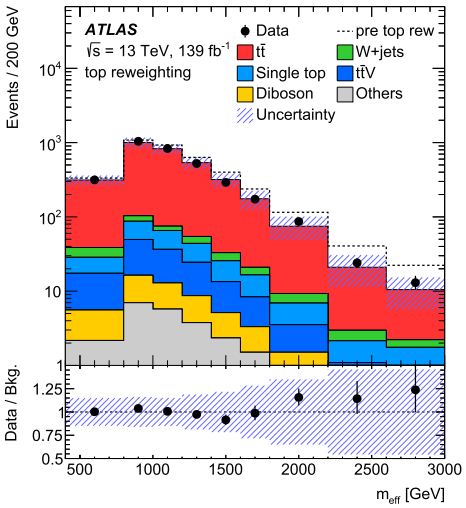

(a)

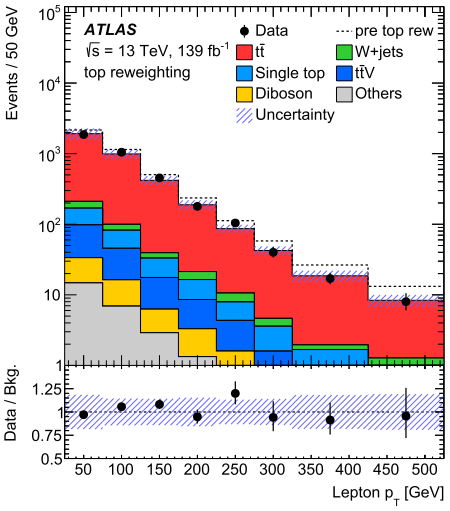

(b)

Fig. 2 Distributions of **a** m_{eff} and **b** lepton p_{T} in the top reweighting region after applying the reweighting factors to the $t\bar{t}$ and single-top background. The dashed line indicates the total background before the reweighting. The band includes statistical and systematic uncertainties. Minor background contributions from $t\bar{t}H$, tWZ, and Z+jets are combined into *Others*. The ratios of the data to the expected background are shown in the bottom panels of the plots. The last bin in each distribution contains the overflow

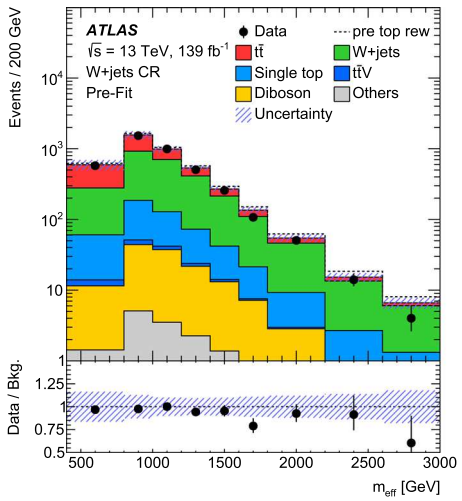

(a)

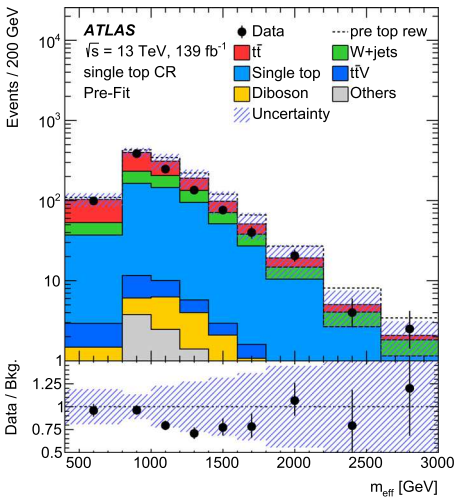

(b)

Fig. 3 Distributions of m_{eff} in **a** the W+jets CR and **b** the single-top CR after applying the top reweighting factors to the simulated $t\bar{t}$ and single-top-quark events. The dashed line indicates the total background before the reweighting. Minor background contributions from $t\bar{t}H$, tWZ, and Z+jets are combined into *Others*. The band includes statistical and systematic uncertainties. The ratios of the data to the expected background are shown in the bottom panels of the plots. The last bin in each distribution contains the overflow

with a positively charged lepton. In the single-top CR, the contribution from W+jets is reduced by requiring at least two b-tagged jets with an angular separation of $\Delta R(b_1, b_2) > 1.4$ between the two highest-p_{T} b-jets. Table 2 summarises the selection criteria for both CRs, and Fig. 3 compares the effective mass distribution in data with that in MC simulation after top reweighting, and also shows the MC expectation before reweighting.

6 Neural network training

To enhance the separation between signal and background events, NNs with several input variables combined into a single discriminant are employed. They are trained for various signal hypotheses using the simulated signal and background events in the training region. For $T\bar{T}$ production, four NNs are trained for different branching ratios $\mathcal{B}(Zt, Ht, Wb)$ covering the region of the branching ratio plane where this analysis is sensitive: (0.8, 0.1, 0.1), (0.2, 0.4, 0.4), (0.4, 0.1, 0.5), (0.4, 0.5, 0.1). Similarly, three NNs are trained for $B\bar{B}$ production, considering the branching ratios $\mathcal{B}(Zb, Hb, Wt) =$ (0.1, 0.1, 0.8), (0.4, 0.1, 0.5), and (0.1, 0.4, 0.5).

The NNs are implemented using the NeuroBayes package [81,82], which combines a three-layer feed-forward NN with preprocessing of the input variables prior to their presentation to the NN. The main purpose of the preprocessing is to facilitate optimal network training by ordering the input variables according to their separation power, taking correlations into account, and removing all but the most relevant ones. Sets of input variables are selected for their ability to discriminate between signal and background. Table 3 lists the input variables that are used to train at least one NN. Each set of input variables is composed of observables reflecting the signal topology, e.g. the high VLQ mass via m_{eff} or the properties of the reclustered large-R jets. Other important variables are the b-jet multiplicity and the transverse masses,

Table 3 Input variables to the NN training, sorted in descending discriminating power between signal and background. The order is not strict as it depends on the VLQ type and branching ratio the NN is trained for

Variable	Description
m_{eff}	Scalar sum of the transverse momenta of leptons, jets, and $E_{\text{T}}^{\text{miss}}$
$N_{b\text{-jets}}$	b-jet multiplicity
m_{T}^{W}	Transverse mass of lepton and $E_{\text{T}}^{\text{miss}}$
am_{T2}	Asymmetric transverse mass
p_{T}(large-R jet$_2$)	Transverse momentum of second-highest-p_{T} large-R jet
$\lvert\Delta\phi(\text{jet}_1, E_{\text{T}}^{\text{miss}})\rvert$	Azimuthal angle between $E_{\text{T}}^{\text{miss}}$ and highest-p_{T} jet
$E_{\text{T}}^{\text{miss}}$	Missing transverse momentum
$\eta(\text{jet}_1)$	Pseudorapidity of highest-p_{T} jet
m(large-R jet$_1$)	Mass of highest-p_{T} large-R jet
N_{const}(large-R jet$_1$)	Number of small-R jets reclustered to the highest-p_{T} large-R jet
$p_{\text{T}}(\ell)$	Transverse momentum of lepton
$p_{\text{T}}(\text{jet}_3)$	Transverse momentum of third-highest-p_{T} jet
$p_{\text{T}}(\text{jet}_2)$	Transverse momentum of second-highest-p_{T} jet

m_{T}^{W} and am_{T2}, that are used to define the CRs and training region. It is checked that all input variables are modelled well. As an example, the distributions of four important input variables in the training region are shown in Fig. 4.

NeuroBayes uses Bayesian regularisation techniques for the training process to improve the generalisation performance and to avoid overtraining. In general, the network infrastructure consists of one input node for each input variable, plus one bias node, an arbitrary, user-defined number of hidden nodes, and one output node which gives a continuous NN output score (NN_{out}) in the interval $(0, +1)$, where NN_{out} values close to zero indicate background-like events and values close to one correspond to signal-like events. For the NNs in this analysis, 15 nodes are used in the hidden layer and the ratio of signal to background events in the training is chosen to be 1:1. The different background processes are weighted according to their expected event contribution. All the main backgrounds, $t\bar{t}$, W+jets, single top quark, and $t\bar{t}V$, are used in the training. For the signal process, VLQ masses from 1 TeV to 1.5 TeV are combined in each training. Events at different signal masses enter with the same cross-section when composing the training sample in order to prevent the lower masses with higher cross-sections from dominating. As a check for potential overtraining, only 80% of the simulated events serve as input to the training, while the remaining 20% are used as a test sample. No signs of overtraining are observed. After the training step, all simulated signal and background events, as well as the observed data events, are processed by the NNs in order to get an NN_{out} value for each event. For each NN, the training region is divided into a low-NN_{out} CR with $NN_{\text{out}} < 0.5$, and the SR with $NN_{\text{out}} > 0.5$.

7 Systematic uncertainties

Several sources of experimental and theoretical systematic uncertainty are considered. The experimental uncertainties are mainly related to the reconstruction and calibration of the final-state physics objects, while the theoretical uncertainties are associated with the modelling of the various processes by the MC event generators. The sources of the largest systematic uncertainties in the analysis are related to the modelling of the major background processes and to the jet energy resolution.

For $t\bar{t}$ and single-top production the following systematic uncertainties related to the event modelling are applied. The uncertainty in the matching procedure between the ME generator and parton shower is assessed by comparing the nominal MadGraph5_aMC@NLO 8 samples with alternative samples generated by MadGraph5_aMC@NLO and showered by Pythia 8. In order to estimate the uncertainties in the modelling of the underlying event, the parton shower, and the hadronisation, the nominal samples are compared with a Powheg+Herwig 7 [83] prediction. Uncertainties related to the choice of renormalisation and factorisation scales of the matrix-element calculation are considered by independently doubling and halving the scales. The impact of initial-state radiation (ISR) is estimated by varying α_{s} in the A14 tune. Similarly, the uncertainty related to final-state radiation (FSR) is assessed by varying the renormalisation scale for final-state parton-shower emissions by a factor of two. The uncertainty related to the choice of scale for the matching of the matrix-element calculation for the $t\bar{t}$ process to the parton shower is evaluated by comparing the nominal samples with an alternative sample produced with the h_{damp} parameter set to $h_{\text{damp}} = 3.0\,m_t$. Uncertainties due to PDFs are obtained using the PDF4LHC15 combined PDF set [84]. A dominant systematic uncertainty in the modelling of the single-top processes stems from the handling of the interference between $t\bar{t}$ and tW at NLO. The uncertainty is estimated by comparing the nominal sample for tW production generated using the diagram-removal scheme with an alternative sample using the diagram-subtraction scheme [45,85]. Finally, an additional 30% normalisation uncertainty is assigned to events from $t\bar{t}$ + heavy-flavour jets production [86].

Uncertainties in the top reweighting procedure arise from the chosen form of the parameterised function and the statistical uncertainties of events in the reweighting region. These are accounted for by varying the parameterised function by $\pm 1\sigma$ from its nominal value, using the uncertainties of the fit parameters and taking their correlations into account. Each

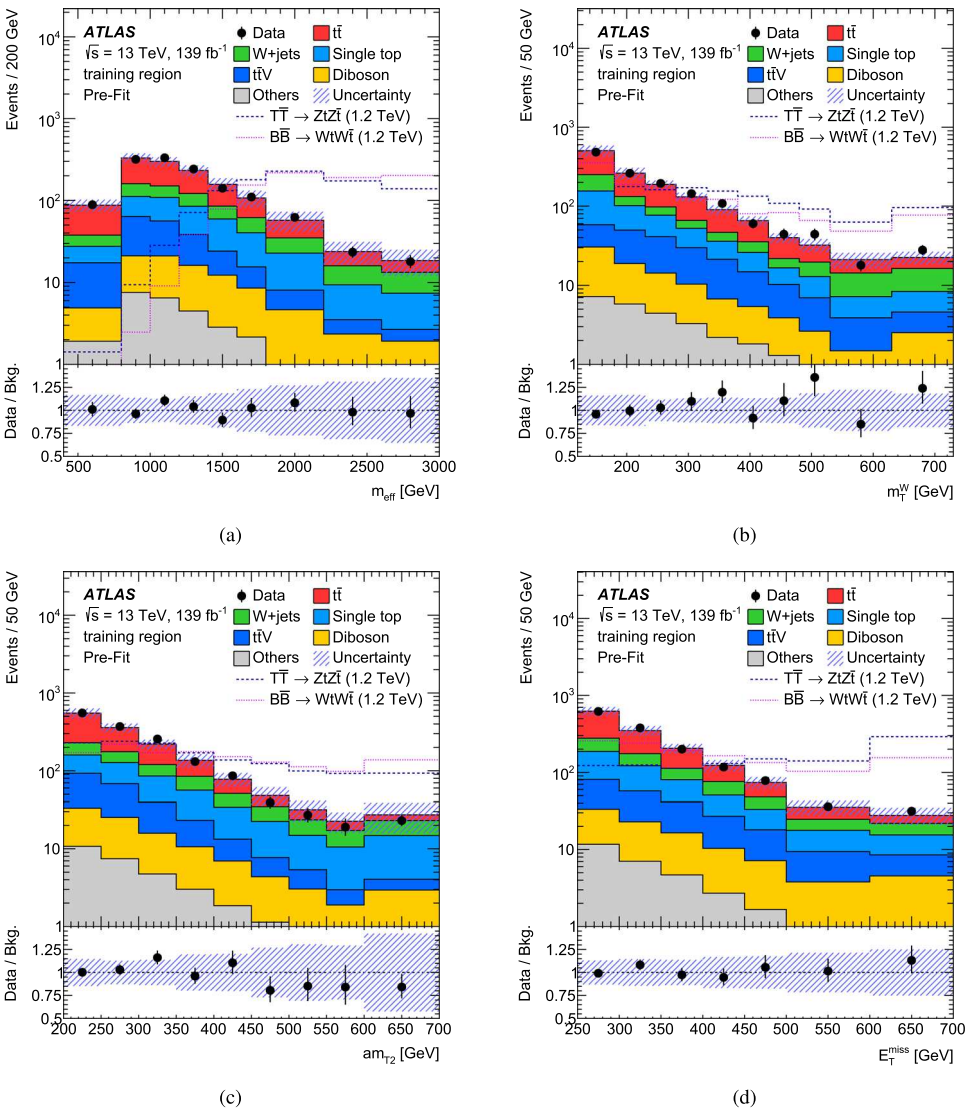

Fig. 4 Distributions of NN input variables in the training region: **a** m_{eff}, **b** m_{T}^{W}, **c** am_{T2} and **d** $E_{\text{T}}^{\text{miss}}$. Minor background contributions from $t\bar{t}H$, tWZ, and Z+jets are combined into *Others*. The signal distributions for $T\bar{T} \to Zt\bar{Z}\bar{t}$ and $B\bar{B} \to WtW\bar{t}$, assuming a VLQ mass of 1.2 TeV, are overlaid and normalised to the total background prediction. The band includes statistical and systematic uncertainties. The ratios of data to the expected background are shown in the bottom panels of the plots. The last bin in each distribution contains the overflow

of the four jet bins for which the reweighting is determined is treated as an independent source of uncertainty.

For all other considered processes, namely V+jets, diboson, $t\bar{t}V$, $t\bar{t}H$, and tWZ production, the renormalisation and factorisation scales are independently varied by a factor of two. A 30% uncertainty is assigned to the heavy-flavour component of the W+jets process, based on a comparison between SHERPA 2.2.1 and data [87].

Backgrounds without a free-floating normalisation parameter in the profile-likelihood fit are assigned a theoretical cross-section uncertainty. For the $t\bar{t}H$ process, an 11% [88] uncertainty is assigned and for $t\bar{t}V$ and tWZ the uncertainty amounts to 15% and 12% [88], respectively. The cross-section uncertainty is taken to be 6% [89] for diboson production and 5% [90] for the Z+jets process.

Besides theoretical systematic uncertainties, detector-related uncertainties are considered in the analysis, the dominant one being the jet energy resolution [68]. Additional jet-related uncertainties are due to the jet energy scale, the jet mass scale and resolution, the efficiency of the JVT requirements, and the b-jet identification [72,91]. Uncertainties associated with leptons arise from the efficiencies of the lepton identification, isolation, and reconstruction, as well as the lepton energy scale and resolution [65,66]. Further experimental uncertainties are related to the scale and resolution of the track soft-term in the $E_{\text{T}}^{\text{miss}}$ calculation [92]. Additional contributions to the total systematic uncertainty come from the uncertainty in the integrated luminosity and the pile-up profile.

8 Statistical analysis

The signal-enriched part of the binned NN output distribution ($NN_{\text{out}} > 0.5$), and the overall number of events in the low-NN_{out}, W+jets, and single-top CRs are used to test for the presence of a signal. For hypothesis testing, binned profile-likelihood fits are performed for each of the seven NNs sep-

arately, following a modified frequentist method [93] implemented in RooStats [94], and taking the systematic uncertainties affecting the signal and background expectations into account as nuisance parameters.

The binned likelihood function $\mathcal{L}(\mu, \theta)$ is constructed as the product of Poisson probability terms over all bins. It depends on the signal strength parameter μ, a factor multiplying the theoretical signal production cross-section, and θ, a set of nuisance parameters, constrained in the likelihood function by Gaussian or log-normal priors. The low-NN_{out}, W+jets, and single-top CRs are used to mainly control the normalisations of $t\bar{t}$, W+jets, and single-top backgrounds, for which additional unconstrained normalisation factors ($\mu_{t\bar{t}}$, $\mu_{W+\text{jets}}$, and $\mu_{\text{single top}}$) are included in the likelihood function. The number of events expected in a bin depends on the normalisation factors as well as on the nuisance parameters. The nuisance parameters θ adjust the expectations for signal and background according to the corresponding systematic uncertainties, and their fitted values correspond to the amounts that best fit the data.

In order to avoid double-counting of normalisation uncertainties for the free-floating background processes, only shape effects and acceptance differences between the CRs and the SR are included when considering the systematic uncertainties in their modelling. A smoothing algorithm is applied to the templates for the systematic variations in case the statistical fluctuations between bins in the signal region are large. Furthermore, the templates for all systematic variations are symmetrised. Some of the dominant systematic uncertainties related to the modelling of the major background processes are one-sided and are symmetrised by mirroring the uncertainty. To simplify the fitting procedure, nuisance parameters are only included for systematic uncertainties that affect the event yield by more than 1% for a process in any bin. Normalisation and shape components for a source of systematic uncertainty are treated separately in this procedure.

The test statistic q_μ is defined as the profile likelihood ratio, $q_\mu = -2\ln \mathcal{L}(\mu, \hat{\hat{\theta}})/\mathcal{L}(\hat{\mu}, \hat{\theta})$, where $\hat{\mu}$ and $\hat{\theta}$ are the values of the parameters that simultaneously maximise the likelihood function, and $\hat{\hat{\theta}}$ are the values of the nuisance parameters that maximise the likelihood function for a fixed value of μ. The compatibility of the observed data with the background-only hypothesis is tested by setting $\mu = 0$ in the test statistic q_0. Upper limits on the signal production cross-section for each considered signal scenario are computed using q_μ in the CL_s method [93] with the asymptotic approximation [95]. A given signal scenario is considered to be excluded at $\geq 95\%$ confidence level (CL) if the value of the signal production cross-section (parameterised by μ) yields a CL_s value ≤ 0.05.

9 Results

Background-only likelihood fits are performed for each NN. The obtained normalisation factors for the $t\bar{t}$, W+jets, and single-top processes vary between the fits for the different NNs: between 1.00 ± 0.28 and 1.14 ± 0.27 for $t\bar{t}$, between 0.91 ± 0.19 and 1.08 ± 0.17 for W+jets, and between 0.53 ± 0.30 and 0.60 ± 0.23 for single top. The reduction of the single-top contribution appears large, but it is less than the difference between the nominal and alternative schemes for modelling the interference between the $t\bar{t}$ and tW processes, which are described in Sects. 3 and 7. The NN_{out} distributions after the fit are validated in the CRs by comparing data with simulation. As an example, the plots for the NN training with a VLT signal with $\mathcal{B}(Zt, Ht, Wb) = (0.8, 0.1, 0.1)$ and a VLB signal with $\mathcal{B}(Zb, Hb, Wt) = (0.1, 0.1, 0.8)$ are shown in Fig. 5. For the training with the VLT signal, the corresponding number of events expected from each process in the three CRs and also the signal region is shown in Table 4, together with the number of observed events and the expected signal yield for a mass of 1.2 TeV. The large uncertainty in the single-top yield due to the different schemes for modeling the interference can also be observed here. The uncertainty in the total background is less than the uncertainty in the separate processes because of strong (anti-)correlations between various systematic uncertainties.

The NN_{out} distributions in the signal region for the two training cases shown in Fig. 5, and for another training for a VLT signal with $\mathcal{B}(Zt, Ht, Wb) = (0.2, 0.4, 0.4)$, are shown in Fig. 6. No significant deviations from the SM expectation are observed for these three cases or when using other trained NNs.

Upper limits on the pair-production cross-sections for T and B quarks are calculated at the 95% CL. For each signal mass and branching ratio, the NN giving the most stringent expected limit is selected. These obtained cross-section limits are compared with the theoretical cross-section to set exclusion limits on the signal mass. The limits are calculated for T and B quarks in the weak-isospin singlet and doublet representations, with mass-dependent branching ratios, as well as for pure $T \to Zt$ and $B \to Wt$ decays, where the latter corresponds to $X \to Wt$ as well as to the (T, B) doublet as mentioned before. For the doublet scenarios, the contribution from the VLQ partner is either not considered, leading to conservative limits, or considered assuming mass-degenerate VLQs. Mass differences of at most a few GeV are allowed, so that decays from one member of the doublet to the other remain suppressed [4,6]. Also for the mass-degenerate doublet scenario the seven NNs described in Sect. 6 are used and the one with the most stringent expected limit is selected as described above, i.e., no additional NN is trained to potentially increase the sensitivity to the added yield from both doublet members.

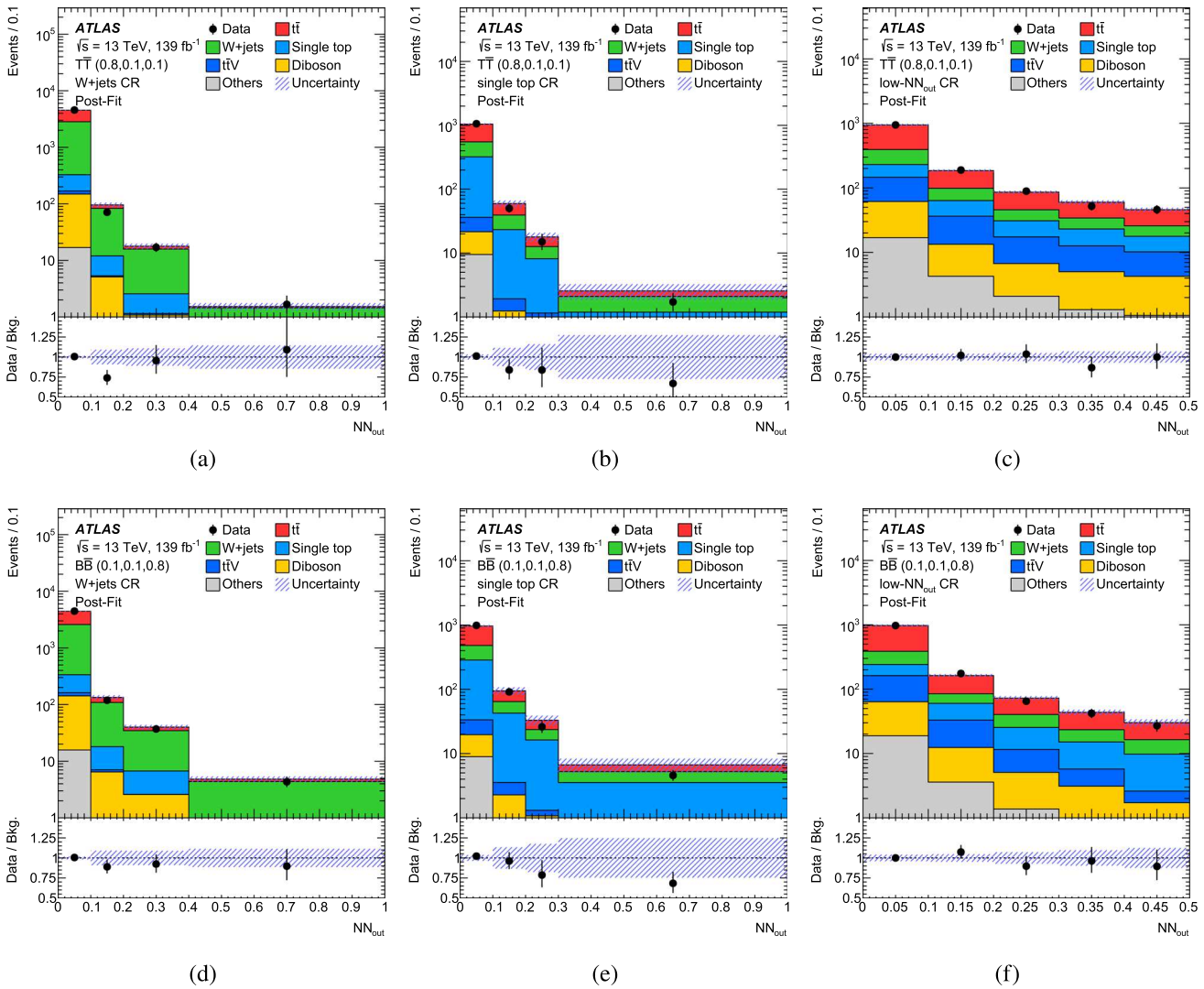

Fig. 5 Data and background expectation in the W+jets CR (left panels), the single-top CR (middle panels), and the low-NN_{out} CR (right panels) after a background-only fit to data (Post-Fit) for a NN training considering a VLT signal with $\mathcal{B}(Zt, Ht, Wb) = (0.8, 0.1, 0.1)$ (upper panels) and a VLB signal with $\mathcal{B}(Zb, Hb, Wt) = (0.1, 0.1, 0.8)$ (lower panels). Minor background contributions from $t\bar{t}H$, tWZ, and Z+jets are combined into *Others*. The band indicates the post-fit uncertainty. The lower panels show the ratio of data to the background expectation

The expected and observed lower limits on the VLQ mass in the aforementioned models are listed in Table 5 and shown in Fig. 7. The impact of the statistical uncertainties on the mass limits is larger than that of the systematic uncertainties. However, the latter is not negligible and for the case of pure $T \to Zt$ ($B \to Wt$) decays it reduces the expected lower limit by about 40 GeV (70 GeV) to a value of 1.45 TeV (1.42 TeV). For the three T-quark scenarios in Table 5, the obtained mass limits are 300–400 GeV higher than in the earlier ATLAS analysis in the same final state using a subset of the Run 2 data [16]. This improvement is only partially due to the larger dataset, as the expected limits on the cross section for a VLT mass of 1.4 TeV improved between a factor of 4.5 for the pure $T \to Zt$ and a factor of 7.7 for the SU(2) singlet. Especially when the branching fraction into Zt becomes smaller the major effect stems from the training of neural networks at several branching ratios instead of using a cut-and-count analysis with a single SR as done previously. The obtained mass limits for the first five scenarios in Table 5 are also better than the corresponding limits in the combination of all ATLAS results using 36 fb^{-1} [26], apart from the T singlet scenario where the observed limit is weaker than the expected limit. The strongest lower limits on the VLQ masses, 1.59 TeV, are derived for the weak-isospin doublets assuming mass-degenerate VLQs.

Apart from limits for specific models and branching ratios, lower limits on the signal mass are set as a function of the T and B branching ratios. The resulting expected and observed

Table 4 Observed data event yields and the expected background event yields with their total uncertainties in the control and signal regions after the background-only fit considering a NN trained for a VLT signal with branching ratio $\mathcal{B}(Zt, Ht, Wb) = (0.8, 0.1, 0.1)$. For comparison, the event yields for a VLT signal with a mass of 1.2 TeV and a branching ratio of $\mathcal{B}(Zt, Ht, Wb) = (0.8, 0.1, 0.1)$ are given

	W+jets CR	Single-top CR	Low-NN_{out} CR	SR
$t\bar{t}$	1720 ± 400	520 ± 130	730 ± 140	79 ± 31
W+jets	2610 ± 370	256 ± 47	231 ± 54	37.7 ± 9.1
Single top	170 ± 150	320 ± 140	143 ± 85	40 ± 30
$t\bar{t}V$	20.4 ± 3.2	15.9 ± 2.6	132 ± 21	23.9 ± 4.0
Diboson	140 ± 17	14.2 ± 2.4	65.4 ± 8.9	12.1 ± 1.8
Z+jets	14.0 ± 3.8	3.85 ± 0.75	4.80 ± 0.73	1.14 ± 0.13
$t\bar{t}H$	2.55 ± 0.33	5.59 ± 0.69	10.9 ± 1.3	2.27 ± 0.33
tWZ	0.90 ± 0.12	0.82 ± 0.11	10.0 ± 1.3	1.89 ± 0.28
Total background	4676 ± 70	1140 ± 34	1322 ± 37	198 ± 14
Data	4676	1135	1321	206
$m_T = 1.2$ TeV				
$\mathcal{B}(Zt, Ht, Wb) = (0.8, 0.1, 0.1)$	0.35 ± 0.12	0.96 ± 0.13	7.01 ± 0.51	53.8 ± 1.8

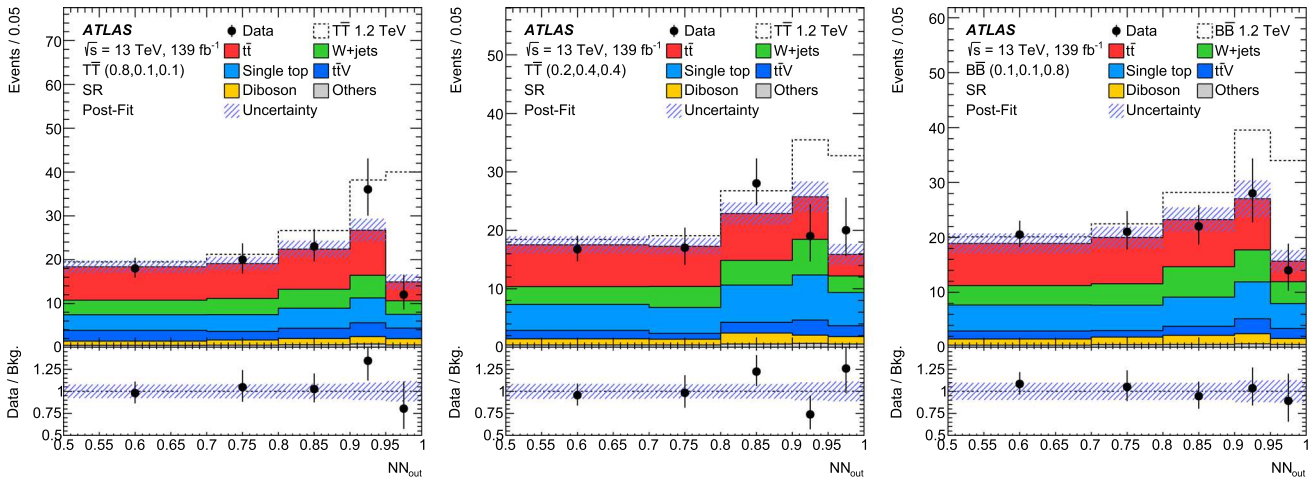

(a) (b) (c)

Fig. 6 Data and background expectation in the signal region after the simultaneous background-only fit to data (Post-Fit) for a NN training for **a** a VLT signal with $\mathcal{B}(Zt, Ht, Wb) = (0.8, 0.1, 0.1)$, **b** a VLT signal with $\mathcal{B}(Zt, Ht, Wb) = (0.2, 0.4, 0.4)$, and **c** a VLB signal with $\mathcal{B}(Zb, Hb, Wt) = (0.1, 0.1, 0.8)$. Contributions from $t\bar{t}H$, tWZ, and Z+jets are combined into *Others*. Expected pre-fit signal distributions with the signal branching ratio corresponding to the respective training are added on top of the background expectation, using a signal mass of 1.2 TeV. The band indicates the statistical and systematic uncertainties. The ratio of data to the background expectation is shown in the bottom panels of the plots

mass limits are shown in Fig. 8. As expected, the highest sensitivity is found in the regions near $\mathcal{B}(T \to Zt) = 100\%$ and $\mathcal{B}(B \to Wt) = 100\%$. For the T quark, the sensitivity for the mixed $ZtHt$ decay mode is larger than for the $ZtWb$ decay. In the case of the B quark, the sensitivity decreases if the branching fraction for B decay into a Higgs or Z boson and a bottom quark increases. The differences between the observed and expected limits for a vector-like T quark around the SU(2) singlet branching ratio are not significant, as can be seen in Fig. 7(c). They result from the NN_{out} distribution obtained from the NN trained for a branching ratio $\mathcal{B}(Zt, Ht, Wb) = (0.2, 0.4, 0.4)$. In the last bin of the corresponding signal region in Fig. 6(b), the data slightly exceeds the predicted SM background.

10 Conclusion

A search for pair-produced vector-like T and B quarks, with electric charge $+2/3$ and $-1/3$, respectively, is performed

Table 5 Expected (Exp.) and observed (Obs.) mass limits for the pair production of specific VLQs (T, B, X) in certain decay scenarios corresponding to SU(2) singlet or doublet representations or to the decay into just one specific final state. In the doublet scenarios, contributions from the VLQ partner are not considered, leading to conservative limits, except for the last row where the VLQs in the doublet are assumed to be mass degenerate. Since the analysis does not distinguish between particles and antiparticles, the limits for $B \to Wt$ also apply to the vector-like X because it decays exclusively into Wt. Similarly, the (T, B) doublet scenarios correspond to (X, T) doublet scenarios

VLQ	Scenario	Exp. limit [TeV]	Obs. limit [TeV]
T	$\mathcal{B}(T \to Zt) = 100\%$	1.45	1.47
T	Singlet	1.33	1.26
T	(T, B) or (X, T) doublet	1.41	1.41
B	Singlet	1.30	1.33
B/X	$\mathcal{B}(B/X \to Wt) = 100\%$ or (T, B)/(X, T) doublet	1.42	1.46
$T/B/X$	(T, B) or (X, T) doublet, mass degenerate	1.56	1.59

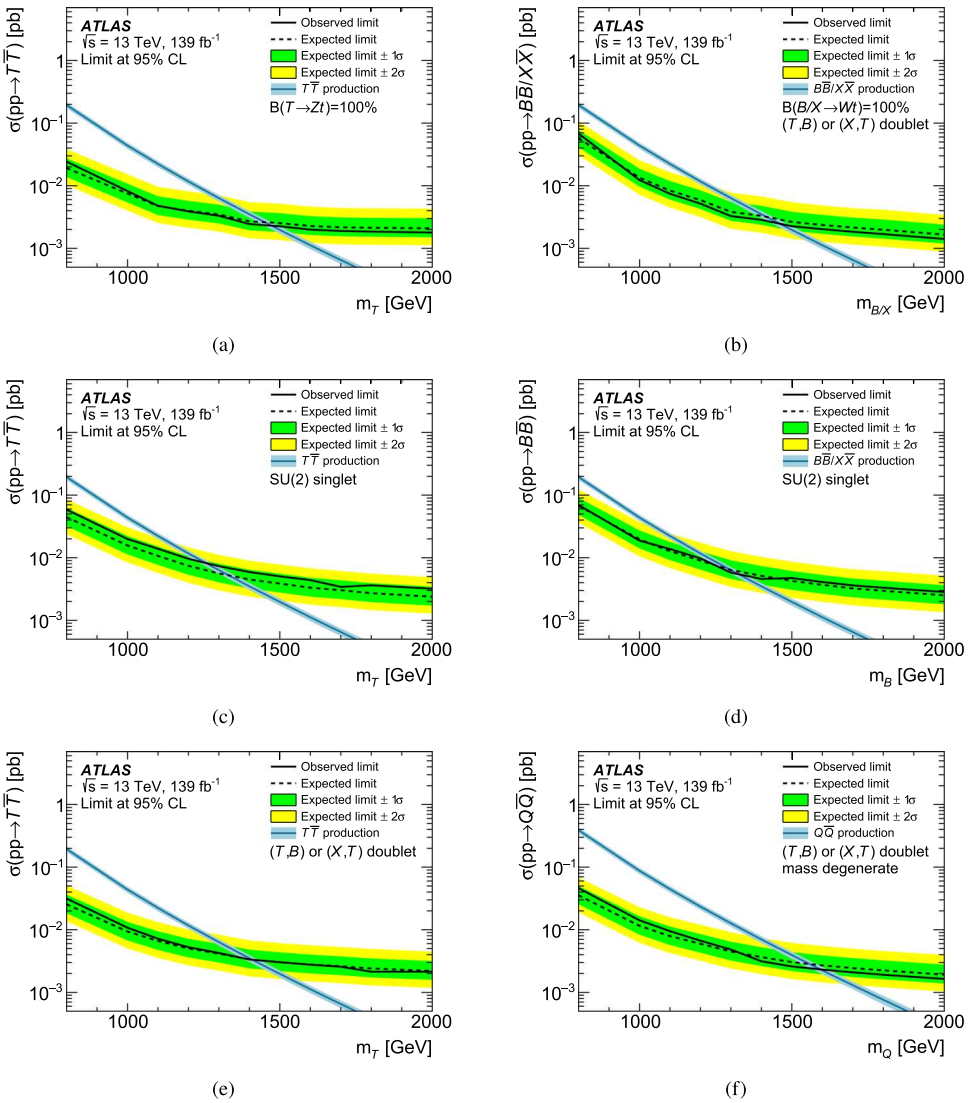

Fig. 7 Expected and observed upper limits on the signal cross-section for **a** the case $\mathcal{B}(T \to Zt) = 100\%$, **b** the case $\mathcal{B}(B \to Wt) = 100\%$, **c** a T quark in the SU(2) singlet representation, **d** a B quark in the SU(2) singlet representation, and **e** a T quark in an SU(2) doublet. In the doublet scenario, contributions from the not-considered vector-like quark are neglected, leading to conservative limits. The SU(2) (T, B) doublet scenario considering contributions from both the T and B quark is shown in (**f**), assuming mass-degenerate VLQs. The thickness of the theory curve represents the theoretical uncertainty from the PDFs, scales, and strong coupling constant α_s

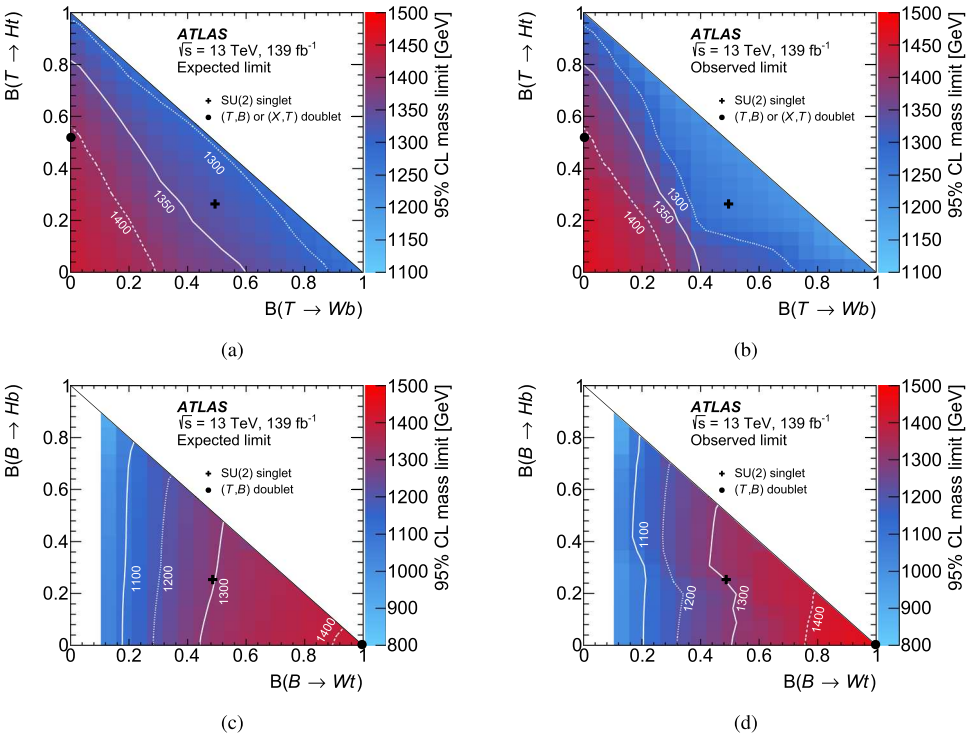

Fig. 8 Expected (left) and observed (right) mass limits for $T\bar{T}$ (upper row) and $B\bar{B}$ (lower row) production. The mass limit is calculated using the NN giving the most stringent expected limit at each signal mass and branching ratio point. The white lines indicate mass exclusion contours. The black markers indicate the branching ratios for the SU(2) singlet and doublet scenarios for masses above 800 GeV, where they are approximately independent of the VLQ mass. Since the analysis does not distinguish between particles and antiparticles, the mass exclusion for the B quark in the (T, B) doublet is equivalent to the exclusion for the X quark in the (X, T) doublet. The white areas indicate that the mass limit is below 800 GeV

in events with exactly one isolated lepton, at least four jets including one that is b-tagged, and high missing transverse momentum. The analysis is based on data collected by the ATLAS experiment in $\sqrt{s} = 13$ TeV proton–proton collisions at the LHC, corresponding to an integrated luminosity of 139fb^{-1}. Several neural networks are trained for various branching ratios of the T and B quarks, assuming decays into a W, Z, or Higgs boson and a third-generation quark. The analysis considers all possible decays of the vector-like quarks, but it is most sensitive to the $T \to Zt$ and $B \to Wt$ decay modes. Since the analysis does not distinguish between particles and antiparticles, the limits for $B \to Wt$ also apply to a vector-like X with electric charge $+5/3$.

No significant deviations from the Standard Model expectation are observed, and 95% CL upper limits on the pair-production cross-sections for T and B quarks as a function of their mass are derived for various decay branching–ratio scenarios. The lower limits on the masses of the T and B quarks in the weak-isospin singlet model are 1.26 TeV and 1.33 TeV, respectively, and 1.41 TeV for the T quark in the doublet representation. For the doublet, the contributions from the VLQ partner are not considered, leading to a conservative limit. Stronger lower limits of 1.47 TeV and 1.46 TeV are set on the masses when considering pure $T \to Zt$ and $B \to Wt$ decays, where the latter corresponds to the (T, B) or (X, T) doublet and also applies to $X \to Wt$ decays. For the three discussed T-quark scenarios, the obtained mass limits are 300 to 400 GeV higher than in the earlier ATLAS analysis in the same final state using a subset of the Run 2 data. The strongest lower limits for T, B and X are at 1.59 TeV for (T, B) and (X, T) weak-isospin doublets where both VLQ partners are considered and assumed to be mass degenerate. Finally, lower limits on the T and B quark masses are derived for all possible branching ratios.

Acknowledgements We thank CERN for the very successful operation of the LHC, as well as the support staff from our institutions without whom ATLAS could not be operated efficiently. We acknowledge the support of ANPCyT, Argentina; YerPhI, Armenia; ARC, Australia; BMWFW and FWF, Austria; ANAS, Azerbaijan; CNPq and FAPESP, Brazil; NSERC, NRC and CFI, Canada; CERN; ANID, Chile; CAS, MOST and NSFC, China; Minciencias, Colombia; MEYS CR, Czech Republic; DNRF and DNSRC, Denmark; IN2P3-CNRS and CEA-DRF/IRFU, France; SRNSFG, Georgia; BMBF, HGF and MPG, Germany; GSRI, Greece; RGC and Hong Kong SAR, China; ISF and Benoziyo Center, Israel; INFN, Italy; MEXT and JSPS, Japan; CNRST, Morocco; NWO, Netherlands; RCN, Norway; MEiN, Poland; FCT, Portugal; MNE/IFA, Romania; MESTD, Serbia; MSSR, Slovakia; ARRS and MIZŠ, Slovenia; DSI/NRF, South Africa; MICINN, Spain; SRC and Wallenberg Foundation, Sweden; SERI, SNSF and Cantons of Bern and Geneva, Switzerland; MOST, Taiwan; TENMAK, Türkiye; STFC, United Kingdom; DOE and NSF, United States of America. In addition, individual groups and members have received support from BCKDF, CANARIE, Compute Canada and CRC, Canada; PRIMUS 21/SCI/017 and UNCE SCI/013, Czech Republic; COST, ERC, ERDF, Horizon 2020 and Marie Skłodowska-Curie Actions, European Union; Investissements d'Avenir Labex, Investissements d'Avenir Idex and ANR, France; DFG and AvH Foundation, Germany; Herakleitos, Thales and Aristeia programmes co-financed by EU-ESF and the Greek NSRF, Greece; BSF-NSF and MINERVA, Israel; Norwegian Financial Mechanism 2014–2021, Norway; NCN and NAWA, Poland; La Caixa Banking Foundation, CERCA Programme Generalitat de Catalunya and PROMETEO and GenT Programmes Generalitat Valenciana, Spain; Göran Gustafssons Stiftelse, Sweden; The Royal Society and Leverhulme Trust, United Kingdom. The crucial computing support from all WLCG partners is acknowledged gratefully, in particular from

CERN, the ATLAS Tier-1 facilities at TRIUMF (Canada), NDGF (Denmark, Norway, Sweden), CC-IN2P3 (France), KIT/GridKA (Germany), INFN-CNAF (Italy), NL-T1 (Netherlands), PIC (Spain), ASGC (Taiwan), RAL (UK) and BNL (USA), the Tier-2 facilities worldwide and large non-WLCG resource providers. Major contributors of computing resources are listed in Ref. [96].

Funded by SCOAP[3]. SCOAP[3] supports the goals of the International Year of Basic Sciences for Sustainable Development.

References

1. L. Susskind, Dynamics of spontaneous symmetry breaking in the Weinberg–Salam theory. Phys. Rev. D **20**, 2619 (1979). https://doi.org/10.1103/PhysRevD.20.2619
2. ATLAS and CMS Collaborations, Combined measurement of the Higgs boson mass in pp collisions at $\sqrt{s} = 7$ and 8 TeV with the ATLAS and CMS experiments. Phys. Rev. Lett. **114**, 191803 (2015). https://doi.org/10.1103/PhysRevLett.114.191803. arXiv:1503.07589 [hep-ex]
3. F. del Aguila, M.J. Bowick, The possibility of new fermions with $\triangle I = 0$ mass. Nucl. Phys. B **224**, 107 (1983). https://doi.org/10.1016/0550-3213(83)90316-4
4. J.A. Aguilar-Saavedra, Identifying top partners at LHC. JHEP **11**, 030 (2009). https://doi.org/10.1088/1126-6708/2009/11/030. arXiv:0907.3155 [hep-ph]
5. Y. Okada, L. Panizzi, LHC signatures of vector-like quarks. Adv. High Energy Phys. **2013**, 364936 (2013). https://doi.org/10.1155/2013/364936. arXiv:1207.5607 [hep-ph]
6. J.A. Aguilar-Saavedra, R. Benbrik, S. Heinemeyer, M. Perez-Victoria, Handbook of vectorlike quarks: mixing and single production. Phys. Rev. D **88**, 094010 (2013). https://doi.org/10.1103/PhysRevD.88.094010. arXiv:1306.0572 [hep-ph]
7. N. Arkani-Hamed, A.G. Cohen, H. Georgi, Electroweak symmetry breaking from dimensional deconstruction. Phys. Lett. B **513**, 232 (2001). https://doi.org/10.1016/S0370-2693(01)00741-9. arXiv:hep-ph/0105239
8. N. Arkani-Hamed, A.G. Cohen, E. Katz, A.E. Nelson, The littlest Higgs. JHEP **07**, 034 (2002). https://doi.org/10.1088/1126-6708/2002/07/034. arXiv:hep-ph/0206021
9. M. Schmaltz, D. Tucker-Smith, Little Higgs theories. Ann. Rev. Nucl. Part. Sci. **55**, 229 (2005). https://doi.org/10.1146/annurev.nucl.55.090704.151502. arXiv:hep-ph/0502182
10. K. Agashe, R. Contino, A. Pomarol, The minimal composite Higgs model. Nucl. Phys. B **719**, 165 (2005). https://doi.org/10.1016/j.nuclphysb.2005.04.035. arXiv:hep-ph/0412089
11. D.B. Kaplan, H. Georgi, S. Dimopoulos, Composite Higgs scalars. Phys. Lett. B **136**, 187 (1984). https://doi.org/10.1016/0370-2693(84)91178-X
12. J.A. Aguilar-Saavedra, Mixing with vector-like quarks: constraints and expectations. EPJ Web Conf. **60**, 16012 (2013). https://doi.org/10.1051/epjconf/20136016012. arXiv:1306.4432 [hep-ph]
13. R. Contino, L. Da Rold, A. Pomarol, Light custodians in natural composite Higgs models. Phys. Rev. D **75**, 055014 (2007). https://doi.org/10.1103/PhysRevD.75.055014. arXiv:hep-ph/0612048
14. ATLAS Collaboration, Search for pair production of up-type vector-like quarks and for four-top-quark events in final states with multiple b-jets with the ATLAS detector. JHEP **07**, 089 (2018). https://doi.org/10.1007/JHEP07(2018)089. arXiv:1803.09678 [hep-ex]
15. ATLAS Collaboration, Search for pair production of heavy vector-like quarks decaying to high-pT W bosons and b quarks in the lepton-plus-jets final state in pp collisions at $\sqrt{s} = 13TeV$ with the ATLAS detector. JHEP **10**, 141 (2017). https://doi.org/10.1007/JHEP10(2017)141. arXiv:1707.03347 [hep-ex]
16. ATLAS Collaboration, Search for pair production of vector-like top quarks in events with one lepton, jets, and missing transverse momentum in $\sqrt{s} = 13TeV$ pp collisions with the ATLAS detector. JHEP **08**, 052 (2017). https://doi.org/10.1007/JHEP08(2017)052. arXiv:1705.10751 [hep-ex]
17. ATLAS Collaboration, Search for new phenomena in events with same-charge leptons and b-jets in pp collisions at $\sqrt{s} = 13TeV$ with the ATLAS detector. JHEP **12**, 039 (2018). https://doi.org/10.1007/JHEP12(2018)039. arXiv:1807.11883 [hep-ex]
18. ATLAS Collaboration, Search for pair- and single-production of vector-like quarks in final states with at least one Z boson decaying into a pair of electrons or muons in pp collision data collected with the ATLAS detector. Phys. Rev. D **98**, 112010 (2018). https://doi.org/10.1103/PhysRevD.98.112010. arXiv:1806.10555 [hep-ex]
19. ATLAS Collaboration, Search for pair production of heavy vector-like quarks decaying into hadronic final states in pp collisions at $\sqrt{s} = 13TeV$ with the ATLAS detector. Phys. Rev. D **98**, 092005 (2018). https://doi.org/10.1103/PhysRevD.98.092005. arXiv:1808.01771 [hep-ex]
20. ATLAS Collaboration, Search for pair production of heavy vector-like quarks decaying into high-p_{T}W bosons and top quarks in the lepton-plus-jets final state in pp collisions at $\sqrt{s} = 13TeV$ with the ATLAS detector. JHEP **08**, 048 (2018). https://doi.org/10.1007/JHEP08(2018)048. arXiv:1806.01762 [hep-ex]
21. ATLAS Collaboration, Search for pair-production of vector-like quarks in pp collision events at $\sqrt{s} = 13TeV$ with at least one leptonically decaying Z boson and a third-generation quark with the ATLAS detector. Phys. Lett. B **843**, 138019 (2023). arXiv:2210.15413 [hep-ex]
22. CMS Collaboration, Search for vector-like T and B quark pairs in final states with leptons at $\sqrt{s} = 13TeV$. JHEP **08**, 177 (2018). https://doi.org/10.1007/JHEP08(2018)177. arXiv:1805.04758 [hep-ex]
23. CMS Collaboration, Search for vector-like quarks in events with two oppositely charged leptons and jets in proton.proton collisions at $\sqrt{s} = 13TeV$. Eur. Phys. J. C **79**, 364 (2019). https://doi.org/10.1140/epjc/s10052-019-6855-8. arXiv:1812.09768 [hep-ex]
24. CMS Collaboration, Search for pair production of vector-like quarks in the $bW\bar{b}W$ channel from proton.proton collisions at $\sqrt{s} = 13TeV$. Phys. Lett. B **779**, 82 (2018). https://doi.org/10.1016/j.physletb.2018.01.077. arXiv:1710.01539 [hep-ex]
25. CMS Collaboration, A search for bottom-type, vector-like quark pair production in a fully hadronic final state in proton.proton collisions at $\sqrt{s} = 13TeV$. Phys. Rev. D **102**, 112004 (2020). https://doi.org/10.1103/PhysRevD.102.112004. arXiv:2008.09835 [hep-ex]
26. ATLAS Collaboration, Combination of the searches for pair-produced vector-like partners of the third-generation quarks at $\sqrt{s} = 13TeV$ with the ATLAS detector. Phys. Rev. Lett. **121**,

211801 (2018). https://doi.org/10.1103/PhysRevLett.121.211801. arXiv:1808.02343 [hep-ex]
27. ATLAS Collaboration, The ATLAS experiment at the CERN large hadron collider. JINST **3**, S08003 (2008). https://doi.org/10.1088/1748-0221/3/08/S08003
28. ATLAS Collaboration, The ATLAS Collaboration Software and Firmware, ATL-SOFT-PUB-2021-001 (2021). https://cds.cern.ch/record/2767187
29. ATLAS Collaboration, ATLAS data quality operations and performance for 2015–2018 data-taking. JINST **15**, P04003 (2020). https://doi.org/10.1088/1748-0221/15/04/P04003. arXiv:1911.04632 [physics.ins-det]
30. ATLAS Collaboration, Luminosity determination in pp collisions at $\sqrt{s} = 13TeV$ using the ATLAS detector at the LHC, ATLAS-CONF-2019-021 (2019). https://cds.cern.ch/record/2677054
31. ATLAS Collaboration, Performance of the missing transverse momentum triggers for the ATLAS detector during Run-2 data taking. JHEP **08**, 080 (2020). https://doi.org/10.1007/JHEP08(2020)080. arXiv:2005.09554 [hep-ex]
32. ATLAS Collaboration, The ATLAS simulation infrastructure. Eur. Phys. J. C **70**, 823 (2010). https://doi.org/10.1140/epjc/s10052-010-1429-9. arXiv:1005.4568 [physics.ins-det]
33. GEANT4 Collaboration, S. Agostinelli et al., GEANT4 — a simulation toolkit. Nucl. Instrum. Methods A **506**, 250 (2003). https://doi.org/10.1016/S0168-9002(03)01368-8
34. T. Sjöstrand, S. Mrenna, P. Skands, A brief introduction to PYTHIA 8.1. Comput. Phys. Commun. **178**, 852 (2008). https://doi.org/10.1016/j.cpc.2008.01.036. arXiv:0710.3820 [hep-ph]
35. ATLAS Collaboration, The Pythia 8 A3 tune description of ATLAS minimum bias and inelastic measurements incorporating the Donnachie-Landshoff diffractive model, ATL-PHYS-PUB-2016-017 (2016). https://cds.cern.ch/record/2206965
36. J.A. Aguilar-Saavedra, PROTOS, a PROgram for TOp Simulations. http://jaguilar.web.cern.ch/jaguilar/protos/
37. R.D. Ball et al., Parton distributions with LHC data. Nucl. Phys. B **867**, 244 (2013). https://doi.org/10.1016/j.nuclphysb.2012.10.003. arXiv:1207.1303 [hep-ph]
38. M. Czakon, A. Mitov, Top++: a program for the calculation of the top-pair cross-section at hadron colliders. Comput. Phys. Commun. **185**, 2930 (2014). https://doi.org/10.1016/j.cpc.2014.06.021. arXiv:1112.5675 [hep-ph]
39. S. Frixione, G. Ridolfi, P. Nason, A positive-weight next-to-leading-order Monte Carlo for heavy flavour hadroproduction. JHEP **09**, 126 (2007). https://doi.org/10.1088/1126-6708/2007/09/126. arXiv:0707.3088 [hep-ph]
40. P. Nason, A new method for combining NLO QCD with shower Monte Carlo algorithms. JHEP **11**, 040 (2004). https://doi.org/10.1088/1126-6708/2004/11/040. arXiv:hep-ph/0409146
41. S. Frixione, P. Nason, C. Oleari, Matching NLO QCD computations with parton shower simulations: the POWHEG method. JHEP **11**, 070 (2007). https://doi.org/10.1088/1126-6708/2007/11/070. arXiv:0709.2092 [hep-ph]
42. S. Alioli, P. Nason, C. Oleari, E. Re, A general framework for implementing NLO calculations in shower Monte Carlo programs: the POWHEG BOX. JHEP **06**, 043 (2010). https://doi.org/10.1007/JHEP06(2010)043. arXiv:1002.2581 [hep-ph]
43. R.D. Ball et al., Parton distributions for the LHC Run II. JHEP **04**, 040 (2015). https://doi.org/10.1007/JHEP04(2015)040. arXiv:1410.8849 [hep-ph]
44. ATLAS Collaboration, Studies on top-quark Monte Carlo modelling for Top2016, ATL-PHYS-PUB-2016-020 (2016). https://cds.cern.ch/record/2216168
45. S. Frixione, E. Laenen, P. Motylinski, C. White, B.R. Webber, Single-top hadroproduction in association with a W boson. JHEP **07**, 029 (2008). https://doi.org/10.1088/1126-6708/2008/07/029. arXiv:0805.3067 [hep-ph]
46. M. Aliev et al., HATHOR-HAdronic Top and Heavy quarks crOss section calculatoR. Comput. Phys. Commun. **182**, 1034 (2011). https://doi.org/10.1016/j.cpc.2010.12.040. arXiv:1007.1327 [hep-ph]
47. P. Kant et al., HatHor for single top-quark production: updated predictions and uncertainty estimates for single top-quark production in hadronic collisions. Comput. Phys. Commun. **74**, 191 (2015). https://doi.org/10.1016/j.cpc.2015.02.001. arXiv:1406.4403 [hep-ph]
48. N. Kidonakis, Two-loop soft anomalous dimensions for single top quark associated production with a W^- or H^-. Phys. Rev. D **82**, 054018 (2010). https://doi.org/10.1103/PhysRevD.82.054018. arXiv:1005.4451 [hep-ph]
49. N. Kidonakis, 'Top Quark Production', Proceedings, Helmholtz International Summer School on Physics of Heavy Quarks and Hadrons (HQ 2013) (JINR, Dubna, Russia, 15th–28th July 2013), p. 139.https://doi.org/10.3204/DESY-PROC-2013-03/Kidonakis. arXiv:1311.0283 [hep-ph]
50. T. Gleisberg, S. Höche, Comix, a new matrix element generator. JHEP **12**, 039 (2008). https://doi.org/10.1088/1126-6708/2008/12/039. arXiv:0808.3674 [hep-ph]
51. F. Buccioni et al., OpenLoops 2. Eur. Phys. J. C **79**, 866 (2019). https://doi.org/10.1140/epjc/s10052-019-7306-2. arXiv:1907.13071 [hep-ph]
52. F. Cascioli, P. Maierhöfer, S. Pozzorini, Scattering amplitudes with open loops. Phys. Rev. Lett. **108**, 111601 (2012). https://doi.org/10.1103/PhysRevLett.108.111601. arXiv:1111.5206 [hep-ph]
53. A. Denner, S. Dittmaier, L. Hofer, Collier: a fortran-based complex one-loop library in extended regularizations. Comput. Phys. Commun. **212**, 220 (2017). https://doi.org/10.1016/j.cpc.2016.10.013. arXiv:1604.06792 [hep-ph]
54. S. Schumann, F. Krauss, A parton shower algorithm based on Catani–Seymour dipole factorisation. JHEP **03**, 038 (2008). https://doi.org/10.1088/1126-6708/2008/03/038. arXiv:0709.1027 [hep-ph]
55. S. Höche, F. Krauss, M. Schönherr, F. Siegert, A critical appraisal of NLO+PS matching methods. JHEP **09**, 049 (2012). https://doi.org/10.1007/JHEP09(2012)049. arXiv:1111.1220 [hep-ph]
56. S. Höche, F. Krauss, M. Schönherr, F. Siegert, QCD matrix elements + parton showers. The NLO case. JHEP **04**, 027 (2013). https://doi.org/10.1007/JHEP04(2013)027. arXiv:1207.5030 [hep-ph]
57. S. Catani, F. Krauss, B.R. Webber, R. Kuhn, QCD matrix elements + parton showers. JHEP **11**, 063 (2001). https://doi.org/10.1088/1126-6708/2001/11/063. arXiv:hep-ph/0109231
58. S. Höche, F. Krauss, S. Schumann, F. Siegert, QCD matrix elements and truncated showers. JHEP **05**, 053 (2009). https://doi.org/10.1088/1126-6708/2009/05/053. arXiv:0903.1219 [hep-ph]
59. C. Anastasiou, L. Dixon, K. Melnikov, F. Petriello, High-precision QCD at hadron colliders: electroweak gauge boson rapidity distributions at next-to-next-to leading order. Phys. Rev. D **69**, 094008 (2004). https://doi.org/10.1103/PhysRevD.69.094008. arXiv:hep-ph/0312266
60. J. Alwall et al., The automated computation of tree-level and next-to-leading order differential cross sections, and their matching to parton shower simulations. JHEP **07**, 079 (2014). https://doi.org/10.1007/JHEP07(2014)079. arXiv:1405.0301 [hep-ph]
61. E. Bothmann et al., Event generation with Sherpa 2.2. SciPost Phys. **7**, 034 (2019). https://doi.org/10.21468/SciPostPhys.7.3.034. arXiv:1905.09127 [hep-ph]
62. D.J. Lange, The EvtGen particle decay simulation package. Nucl. Instrum. Methods A **462**, 152 (2001). https://doi.org/10.1016/S0168-9002(01)00089-4
63. T. Sjöstrand et al., An introduction to PYTHIA 8.2. Comput. Phys. Commun. **191**, 159 (2015). https://doi.org/10.1016/j.cpc.2015.01.024. arXiv:1410.3012 [hep-ph]

64. ATLAS Collaboration, ATLAS Pythia 8 tunes to 7 TeV data, ATL-PHYS-PUB-2014-021 (2014). https://cds.cern.ch/record/1966419
65. ATLAS Collaboration, Electron and photon performance measurements with the ATLAS detector using the 2015-2017 LHC proton.proton collision data. JINST **14**, P12006 (2019). https://doi.org/10.1088/1748-0221/14/12/P12006. arXiv:1908.00005 [hep-ex]
66. ATLAS Collaboration, Muon reconstruction and identification efficiency in ATLAS using the full Run 2 pp collision data set at $\sqrt{3} = 13TeV$. Eur. Phys. J. C **81**, 578 (2021). https://doi.org/10.1140/epjc/s10052-021-09233-2. arXiv:2012.00578 [hep-ex]
67. ATLAS Collaboration, Jet reconstruction and performance using particle flow with the ATLAS Detector. Eur. Phys. J. C **77**, 466 (2017).https://doi.org/10.1140/epjc/s10052-017-5031-2. arXiv:1703.10485 [hep-ex]
68. ATLAS Collaboration, Jet energy scale and resolution measured in proton-proton collisions at $\sqrt{3} = 13TeV$ with the ATLAS detector. Eur. Phys. J. C **81**, 689 (2020). https://doi.org/10.1140/epjc/s10052-021-09402-3. arXiv:2007.02645 [hep-ex]
69. M. Cacciari, G.P. Salam, G. Soyez, The anti-k_t jet clustering algorithm. JHEP **04**, 063 (2008). https://doi.org/10.1088/1126-6708/2008/04/063. arXiv:0802.1189 [hep-ph]
70. M. Cacciari, G.P. Salam, G. Soyez, FastJet user manual. Eur. Phys. J. C **72**, 1896 (2012). https://doi.org/10.1140/epjc/s10052-012-1896-2. arXiv:1111.6097 [hep-ph]
71. ATLAS Collaboration, Tagging and suppression of pileup jets with the ATLAS detector, ATLAS-CONF-2014-018 (2014). https://cds.cern.ch/record/1700870
72. ATLAS Collaboration, ATLAS b-jet identification performance and efficiency measurement with $t\bar{t}$ events in pp collisions at $\sqrt{3} = 13TeV$. Eur. Phys. J. C **79**, 970 (2019). https://doi.org/10.1140/epjc/s10052-019-7450-8. arXiv:1907.05120 [hep-ex]
73. ATLAS Collaboration, ATLAS flavour-tagging algorithms for the LHC Run 2 pp collision dataset (2022). arXiv: 2211.16345 [physics.data-an]
74. ATLAS Collaboration, Performance of missing transverse momentum reconstruction with the ATLAS detector using proton-proton collisions at $\sqrt{3} = 13TeV$. Eur. Phys. J. C **78**, 903 (2018). https://doi.org/10.1140/epjc/s10052-018-6288-9. arXiv:1802.08168 [hep-ex]
75. P. Konar, K. Kong, K.T. Matchev, M. Park, Dark matter particle spectroscopy at the LHC: generalizing M(T2) to asymmetric event topologies. JHEP **04**, 086 (2010). https://doi.org/10.1007/JHEP04(2010)086. arXiv:0911.4126 [hep-ph]
76. C.G. Lester, B. Nachman, Bisection-based asymmetric M_{T2} computation: a higher precision calculator than existing symmetric methods. JHEP **03**, 100 (2015). https://doi.org/10.1007/JHEP03(2015)100. arXiv:1411.4312 [hep-ph]
77. C.G. Lester, D.J. Summers, Measuring masses of semiinvisibly decaying particles pair produced at hadron colliders. Phys. Lett. B **463**, 99 (1999). https://doi.org/10.1016/S0370-2693(99)00945-4. arXiv:hep-ph/9906349
78. A. Barr, C. Lester, P. Stephens, m(T2): the truth behind the glamour. J. Phys. G **29**, 2343 (2003). https://doi.org/10.1088/0954-3899/29/10/304. arXiv:hep-ph/0304226
79. ATLAS Collaboration, Measurement of the $t\bar{t}$ production cross-section and lepton differential distributions in $e\mu$ dilepton events from pp collisions at $\sqrt{3} = 13TeV$ with the ATLAS detector. Eur. Phys. J. C **80**, 528 (2020). https://doi.org/10.1140/epjc/s10052-020-7907-9. arXiv:1910.08819 [hep-ex]
80. ATLAS Collaboration, Measurements of top-quark pair differential and double-differential cross-sections in the $\ell+$ jets channel with pp collisions at $\sqrt{3} = 13TeV$ using the ATLAS detector. Eur. Phys. J. C **79**, 1028 (2019).https://doi.org/10.1140/epjc/s10052-019-7525-6. arXiv:1908.07305 [hep-ex]. Erratum: Eur. Phys. J. C **80**, 1092 (2020)
81. M. Feindt, A Neural Bayesian Estimator for Conditional Probability Densities (2004). arXiv:physics/0402093 [physics.data-an]
82. M. Feindt, U. Kerzel, The NeuroBayes neural network package. Nucl. Instrum. Methods A **559**, 190 (2006). https://doi.org/10.1016/j.nima.2005.11.166
83. J. Bellm et al., Herwig 7.1 Release Note (2017). arXiv:1705.06919 [hep-ph]
84. J. Butterworth et al., PDF4LHC recommendations for LHC Run II. J. Phys. G **43**, 023001 (2016). https://doi.org/10.1088/0954-3899/43/2/023001. arXiv:1510.03865 [hep-ph]
85. E. Re, Single-top Wt-channel production matched with parton showers using the POWHEG method. Eur. Phys. J. C **71**, 1547 (2011). https://doi.org/10.1140/epjc/s10052-011-1547-z. arXiv:1009.2450 [hep-ph]
86. ATLAS Collaboration, Search for the standard model Higgs boson produced in association with top quarks and decaying into a $b\bar{b}$ pair in pp collisions at $\sqrt{3} = 13TeV$ with the ATLAS detector. Phys. Rev. D **97**, 072016 (2018).https://doi.org/10.1103/PhysRevD.97.072016. arXiv:1712.08895 [hep-ex]
87. ATLAS Collaboration, Measurements of WH and ZH production in the $H \to b\bar{b}$ decay channel in pp collisions at 13 TeV with the ATLAS detector. Eur. Phys. J. C **81**, 178 (2021). https://doi.org/10.1140/epjc/s10052-020-08677-2. arXiv:2007.02873 [hep-ex]
88. D. de Florian et al., Handbook of LHC Higgs Cross Sections: 4. Deciphering the Nature of the Higgs Sector (2016). https://doi.org/10.23731/CYRM-2017-002. arXiv:1610.07922 [hep-ph]
89. ATLAS Collaboration, Multi-boson simulation for 13 TeV ATLAS analyses, ATL-PHYS-PUB-2016-002 (2016). https://cds.cern.ch/record/2119986
90. ATLAS Collaboration, Measurement of $W\pm$ and Z-boson production cross sections in pp collisions at $\sqrt{3} = 13TeV$ with the ATLAS detector. Phys. Lett. B **759**, 601 (2016).https://doi.org/10.1016/j.physletb.2016.06.023. arXiv:1603.09222 [hep-ex]
91. ATLAS Collaboration, Measurement of the c-jet mistagging efficiency in $t\bar{t}$ events using pp collision data at $\sqrt{3} = 13TeV$ collected with the ATLAS detector. Eur. Phys. J. C **82**, 95 (2021). https://doi.org/10.1140/epjc/s10052-021-09843-w. arXiv:2109.10627 [hep-ex]
92. ATLAS Collaboration, E_T^{miss} performance in the ATLAS detector using 2015.2016 LHC pp collisions, ATLAS-CONF-2018-023 (2018). https://cds.cern.ch/record/2625233
93. A.L. Read, Presentation of search results: the CL_S technique. J. Phys. G **28**, 2693 (2002). https://doi.org/10.1088/0954-3899/28/10/313
94. W. Verkerke, D. Kirkby, The RooFit toolkit for data modeling (2003). arXiv:physics/0306116 [physics.data-an]
95. G. Cowan, K. Cranmer, E. Gross, O. Vitells, Asymptotic formulae for likelihood-based tests of new physics. Eur. Phys. J. C **71**, 1554 (2011). https://doi.org/10.1140/epjc/s10052-011-1554-0. arXiv:1007.1727 [physics.data-an]. Erratum: Eur. Phys. J. C **73**, 2501 (2013)
96. ATLAS Collaboration, ATLAS Computing Acknowledgements, ATL-SOFT-PUB-2021-003. https://cds.cern.ch/record/2776662

ATLAS Collaboration*

G. Aad[101], B. Abbott[119], D. C. Abbott[102], K. Abeling[55], S. H. Abidi[29], A. Aboulhorma[35e], H. Abramowicz[150], H. Abreu[149], Y. Abulaiti[116], A. C. Abusleme Hoffman[136a], B. S. Acharya[68a,68b,p], C. Adam Bourdarios[4], L. Adamczyk[84a], L. Adamek[154], S. V. Addepalli[26], J. Adelman[114], A. Adiguzel[21c], S. Adorni[56], T. Adye[133], A. A. Affolder[135], Y. Afik[36], M. N. Agaras[13], J. Agarwala[72a,72b], A. Aggarwal[99], C. Agheorghiesei[27c], J. A. Aguilar-Saavedra[129f], A. Ahmad[36], F. Ahmadov[38,z], W. S. Ahmed[103], S. Ahuja[94], X. Ai[48], G. Aielli[75a,75b], I. Aizenberg[168], M. Akbiyik[99], T. P. A. Åkesson[97], A. V. Akimov[37], K. Al Khoury[41], G. L. Alberghi[23b], J. Albert[164], P. Albicocco[53], S. Alderweireldt[52], M. Aleksa[36], I. N. Aleksandrov[38], C. Alexa[27b], T. Alexopoulos[10], A. Alfonsi[113], F. Alfonsi[23b], M. Alhroob[119], B. Ali[131], S. Ali[147], M. Aliev[37], G. Alimonti[70a], W. Alkakhi[55], C. Allaire[66], B. M. M. Allbrooke[145], C. A. Allendes Flores[136f], P. P. Allport[20], A. Aloisio[71a,71b], F. Alonso[89], C. Alpigiani[137], E. Alunno Camelia[75a,75b], M. Alvarez Estevez[98], M. G. Alviggi[71a,71b], M. Aly[100], Y. Amaral Coutinho[81b], A. Ambler[103], C. Amelung[36], M. Amerl[1], C. G. Ames[108], D. Amidei[105], S. P. Amor Dos Santos[129a], S. Amoroso[48], K. R. Amos[162], V. Ananiev[124], C. Anastopoulos[138], T. Andeen[11], J. K. Anders[36], S. Y. Andrean[47a,47b], A. Andreazza[70a,70b], S. Angelidakis[9], A. Angerami[41,ab], A. V. Anisenkov[37], A. Annovi[73a], C. Antel[56], M. T. Anthony[138], E. Antipov[120], M. Antonelli[53], D. J. A. Antrim[17a], F. Anulli[74a], M. Aoki[82], T. Aoki[152], J. A. Aparisi Pozo[162], M. A. Aparo[145], L. Aperio Bella[48], C. Appelt[18], N. Aranzabal[36], V. Araujo Ferraz[81a], C. Arcangeletti[53], A. T. H. Arce[51], E. Arena[91], J-F. Arguin[107], S. Argyropoulos[54], J.-H. Arling[48], A. J. Armbruster[36], O. Arnaez[154], H. Arnold[113], Z. P. Arrubarrena Tame[108], G. Artoni[74a,74b], H. Asada[110], K. Asai[117], S. Asai[152], N. A. Asbah[61], J. Assahsah[35d], K. Assamagan[29], R. Astalos[28a], R. J. Atkin[33a], M. Atkinson[161], N. B. Atlay[18], H. Atmani[62b], P. A. Atmasiddha[105], K. Augsten[131], S. Auricchio[71a,71b], A. D. Auriol[20], V. A. Austrup[170], G. Avner[149], G. Avolio[36], K. Axiotis[56], M. K. Ayoub[14c], G. Azuelos[107,ae], D. Babal[28a], H. Bachacou[134], K. Bachas[151,r], A. Bachiu[34], F. Backman[47a,47b], A. Badea[61], P. Bagnaia[74a,74b], M. Bahmani[18], A. J. Bailey[162], V. R. Bailey[161], J. T. Baines[133], C. Bakalis[10], O. K. Baker[171], P. J. Bakker[113], E. Bakos[15], D. Bakshi Gupta[8], S. Balaji[146], R. Balasubramanian[113], E. M. Baldin[37], P. Balek[132], E. Ballabene[70a,70b], F. Balli[134], L. M. Baltes[63a], W. K. Balunas[32], J. Balz[99], E. Banas[85], M. Bandieramonte[128], A. Bandyopadhyay[24], S. Bansal[24], L. Barak[150], E. L. Barberio[104], D. Barberis[57a,57b], M. Barbero[101], G. Barbour[95], K. N. Barends[33a], T. Barillari[109], M-S. Barisits[36], T. Barklow[142], R. M. Barnett[17a], P. Baron[121], D. A. Baron Moreno[100], A. Baroncelli[62a], G. Barone[29], A. J. Barr[125], L. Barranco Navarro[47a,47b], F. Barreiro[98], J. Barreiro Guimarães da Costa[14a], U. Barron[150], M. G. Barros Teixeira[129a], S. Barsov[37], F. Bartels[63a], R. Bartoldus[142], A. E. Barton[90], P. Bartos[28a], A. Basalaev[48], A. Basan[99], M. Baselga[49], I. Bashta[76a,76b], A. Bassalat[66,ak], M. J. Basso[154], C. R. Basson[100], R. L. Bates[59], S. Batlamous[35e], J. R. Batley[32], B. Batool[140], M. Battaglia[135], D. Battulga[18], M. Bauce[74a,74b], P. Bauer[24], A. Bayirli[21a], J. B. Beacham[51], T. Beau[126], P. H. Beauchemin[157], F. Becherer[54], P. Bechtle[24], H. P. Beck[19,q], K. Becker[166], A. J. Beddall[21d], V. A. Bednyakov[38], C. P. Bee[144], L. J. Beemster[15], T. A. Beermann[36], M. Begalli[81d], M. Begel[29], A. Behera[144], J. K. Behr[48], C. Beirao Da Cruz E Silva[36], J. F. Beirer[36,55], F. Beisiegel[24], M. Belfkir[158], G. Bella[150], L. Bellagamba[23b], A. Bellerive[34], P. Bellos[20], K. Beloborodov[37], K. Belotskiy[37], N. L. Belyaev[37], D. Benchekroun[35a], F. Bendebba[35a], Y. Benhammou[150], D. P. Benjamin[29], M. Benoit[29], J. R. Bensinger[26], S. Bentvelsen[113], L. Beresford[36], M. Beretta[53], E. Bergeaas Kuutmann[160], N. Berger[4], B. Bergmann[131], J. Beringer[17a], S. Berlendis[7], G. Bernardi[5], C. Bernius[142], F. U. Bernlochner[24], T. Berry[94], P. Berta[132], A. Berthold[50], I. A. Bertram[90], S. Bethke[109], A. Betti[74a,74b], A. J. Bevan[93], M. Bhamjee[33c], S. Bhatta[144], D. S. Bhattacharya[165], P. Bhattarai[26], V. S. Bhopatkar[120], R. Bi[29,ah], R. M. Bianchi[128], O. Biebel[108], R. Bielski[122], M. Biglietti[76a], T. R. V. Billoud[131], M. Bindi[55], A. Bingul[21b], C. Bini[74a,74b], A. Biondini[91], C. J. Birch-sykes[100], G. A. Bird[20,133], M. Birman[168], T. Bisanz[36], E. Bisceglie[43a,43b], D. Biswas[169,l], A. Bitadze[100], K. Bjørke[124], I. Bloch[48], C. Blocker[26], A. Blue[59], U. Blumenschein[93], J. Blumenthal[99], G. J. Bobbink[113], V. S. Bobrovnikov[37], M. Boehler[54], D. Bogavac[36], A. G. Bogdanchikov[37], C. Bohm[47a], V. Boisvert[94], P. Bokan[48], T. Bold[84a], M. Bomben[5], M. Bona[93], M. Boonekamp[134], C. D. Booth[94], A. G. Borbély[59], H. M. Borecka-Bielska[107], L. S. Borgna[95], G. Borissov[90], D. Bortoletto[125], D. Boscherini[23b], M. Bosman[13], J. D. Bossio Sola[36], K. Bouaouda[35a], N. Bouchhar[162], J. Boudreau[128], E. V. Bouhova-Thacker[90], D. Boumediene[40], R. Bouquet[5], A. Boveia[118], J. Boyd[36], D. Boye[29], I. R. Boyko[38], J. Bracinik[20], N. Brahimi[62d], G. Brandt[170], O. Brandt[32],

F. Braren[48], B. Brau[102], J. E. Brau[122], K. Brendlinger[48], R. Brener[168], L. Brenner[113], R. Brenner[160], S. Bressler[168], D. Britton[59], D. Britzger[109], I. Brock[24], G. Brooijmans[41], W. K. Brooks[136f], E. Brost[29], T. L. Bruckler[125], P. A. Bruckman de Renstrom[85], B. Brüers[48], D. Bruncko[28b,*], A. Bruni[23b], G. Bruni[23b], M. Bruschi[23b], N. Bruscino[74a,74b], T. Buanes[16], Q. Buat[137], P. Buchholz[140], A. G. Buckley[59], I. A. Budagov[38,*], M. K. Bugge[124], O. Bulekov[37], B. A. Bullard[142], S. Burdin[91], C. D. Burgard[49], A. M. Burger[40], B. Burghgrave[8], J. T. P. Burr[32], C. D. Burton[11], J. C. Burzynski[141], E. L. Busch[41], V. Büscher[99], P. J. Bussey[59], J. M. Butler[25], C. M. Buttar[59], J. M. Butterworth[95], W. Buttinger[133], C. J. Buxo Vazquez[106], A. R. Buzykaev[37], G. Cabras[23b], S. Cabrera Urbán[162], D. Caforio[58], H. Cai[128], Y. Cai[14a,14d], V. M. M. Cairo[36], O. Cakir[3a], N. Calace[36], P. Calafiura[17a], G. Calderini[126], P. Calfayan[67], G. Callea[59], L. P. Caloba[81b], D. Calvet[40], S. Calvet[40], T. P. Calvet[101], M. Calvetti[73a,73b], R. Camacho Toro[126], S. Camarda[36], D. Camarero Munoz[26], P. Camarri[75a,75b], M. T. Camerlingo[71a,71b], D. Cameron[124], C. Camincher[164], M. Campanelli[95], A. Camplani[42], V. Canale[71a,71b], A. Canesse[103], M. Cano Bret[79], J. Cantero[162], Y. Cao[161], F. Capocasa[26], M. Capua[43a,43b], A. Carbone[70a,70b], R. Cardarelli[75a], J. C. J. Cardenas[8], F. Cardillo[162], T. Carli[36], G. Carlino[71a], J. I. Carlotto[13], B. T. Carlson[128,s], E. M. Carlson[155a,164], L. Carminati[70a,70b], M. Carnesale[74a,74b], S. Caron[112], E. Carquin[136f], S. Carrá[70a,70b], G. Carratta[23a,23b], F. Carrio Argos[33g], J. W. S. Carter[154], T. M. Carter[52], M. P. Casado[13,i], A. F. Casha[154], E. G. Castiglia[171], F. L. Castillo[63a], L. Castillo Garcia[13], V. Castillo Gimenez[162], N. F. Castro[129a,129e], A. Catinaccio[36], J. R. Catmore[124], V. Cavaliere[29], N. Cavalli[23a,23b], V. Cavasinni[73a,73b], E. Celebi[21a], F. Celli[125], M. S. Centonze[69a,69b], K. Cerny[121], A. S. Cerqueira[81a], A. Cerri[145], L. Cerrito[75a,75b], F. Cerutti[17a], A. Cervelli[23b], S. A. Cetin[21d], Z. Chadi[35a], D. Chakraborty[114], M. Chala[129f], J. Chan[169], W. Y. Chan[152], J. D. Chapman[32], B. Chargeishvili[148b], D. G. Charlton[20], T. P. Charman[93], M. Chatterjee[19], S. Chekanov[6], S. V. Chekulaev[155a], G. A. Chelkov[38,a], A. Chen[105], B. Chen[150], B. Chen[164], H. Chen[14c], H. Chen[29], J. Chen[62c], J. Chen[141], S. Chen[152], S. J. Chen[14c], X. Chen[62c], X. Chen[14b,ad], Y. Chen[62a], C. L. Cheng[169], H. C. Cheng[64a], S. Cheong[142], A. Cheplakov[38], E. Cheremushkina[48], E. Cherepanova[113], R. Cherkaoui El Moursli[35e], E. Cheu[7], K. Cheung[65], L. Chevalier[134], V. Chiarella[53], G. Chiarelli[73a], N. Chiedde[101], G. Chiodini[69a], A. S. Chisholm[20], A. Chitan[27b], M. Chitishvili[162], Y. H. Chiu[164], M. V. Chizhov[38], K. Choi[11], A. R. Chomont[74a,74b], Y. Chou[102], E. Y. S. Chow[113], T. Chowdhury[33g], L. D. Christopher[33g], K. L. Chu[64a], M. C. Chu[64a], X. Chu[14a,14d], J. Chudoba[130], J. J. Chwastowski[85], D. Cieri[109], K. M. Ciesla[84a], V. Cindro[92], A. Ciocio[17a], F. Cirotto[71a,71b], Z. H. Citron[168,m], M. Citterio[70a], D. A. Ciubotaru[27b], B. M. Ciungu[154], A. Clark[56], P. J. Clark[52], J. M. Clavijo Columbie[48], S. E. Clawson[100], C. Clement[47a,47b], J. Clercx[48], L. Clissa[23a,23b], Y. Coadou[101], M. Cobal[68a,68c], A. Coccaro[57b], R. F. Coelho Barrue[129a], R. Coelho Lopes De Sa[102], S. Coelli[70a], H. Cohen[150], A. E. C. Coimbra[70a,70b], B. Cole[41], J. Collot[60], P. Conde Muiño[129a,129g], M. P. Connell[33c], S. H. Connell[33c], I. A. Connelly[59], E. I. Conroy[125], F. Conventi[71a,af], H. G. Cooke[20], A. M. Cooper-Sarkar[125], F. Cormier[163], L. D. Corpe[36], M. Corradi[74a,74b], E. E. Corrigan[97], F. Corriveau[103,x], A. Cortes-Gonzalez[18], M. J. Costa[162], F. Costanza[4], D. Costanzo[138], B. M. Cote[118], G. Cowan[94], J. W. Cowley[32], K. Cranmer[116], S. Crépé-Renaudin[60], F. Crescioli[126], M. Cristinziani[140], M. Cristoforetti[77a,77b,c], V. Croft[157], G. Crosetti[43a,43b], A. Cueto[36], T. Cuhadar Donszelmann[159], H. Cui[14a,14d], Z. Cui[7], W. R. Cunningham[59], F. Curcio[43a,43b], P. Czodrowski[36], M. M. Czurylo[63b], M. J. Da Cunha Sargedas De Sousa[62a], J. V. Da Fonseca Pinto[81b], C. Da Via[100], W. Dabrowski[84a], T. Dado[49], S. Dahbi[33g], T. Dai[105], C. Dallapiccola[102], M. Dam[42], G. D'amen[29], V. D'Amico[108], J. Damp[99], J. R. Dandoy[127], M. F. Daneri[30], M. Danninger[141], V. Dao[36], G. Darbo[57b], S. Darmora[6], S. J. Das[29,al], S. D'Auria[70a,70b], C. David[155b], T. Davidek[132], D. R. Davis[51], B. Davis-Purcell[34], I. Dawson[93], K. De[8], R. De Asmundis[71a], M. De Beurs[113], N. De Biase[48], S. De Castro[23a,23b], N. De Groot[112], P. de Jong[113], H. De la Torre[106], A. De Maria[14c], A. De Salvo[74a], U. De Sanctis[75a,75b], A. De Santo[145], J. B. De Vivie De Regie[60], D. V. Dedovich[38], J. Degens[113], A. M. Deiana[44], F. Del Corso[23a,23b], J. Del Peso[98], F. Del Rio[63a], F. Deliot[134], C. M. Delitzsch[49], M. Della Pietra[71a,71b], D. Della Volpe[56], A. Dell'Acqua[36], L. Dell'Asta[70a,70b], M. Delmastro[4], P. A. Delsart[60], S. Demers[171], M. Demichev[38], S. P. Denisov[37], L. D'Eramo[114], D. Derendarz[85], F. Derue[126], P. Dervan[91], K. Desch[24], K. Dette[154], C. Deutsch[24], F. A. Di Bello[57a,57b], A. Di Ciaccio[75a,75b], L. Di Ciaccio[4], A. Di Domenico[74a,74b], C. Di Donato[71a,71b], A. Di Girolamo[36], G. Di Gregorio[5], A. Di Luca[77a,77b], B. Di Micco[76a,76b], R. Di Nardo[76a,76b], C. Diaconu[101], F. A. Dias[113], T. Dias Do Vale[141], M. A. Diaz[136a,136b], F. G. Diaz Capriles[24], M. Didenko[162], E. B. Diehl[105], L. Diehl[54], S. Díez Cornell[48], C. Diez Pardos[140], C. Dimitriadi[24,160], A. Dimitrievska[17a], J. Dingfelder[24], I-M. Dinu[27b], S. J. Dittmeier[63b], F. Dittus[36],

F. Djama[101], T. Djobava[148b], J. I. Djuvsland[16], C. Doglioni[97,100], J. Dolejsi[132], Z. Dolezal[132], M. Donadelli[81c], B. Dong[106], J. Donini[40], A. D'Onofrio[76a,76b], M. D'Onofrio[91], J. Dopke[133], A. Doria[71a], M. T. Dova[89], A. T. Doyle[59], M. A. Draguet[125], E. Drechsler[141], E. Dreyer[168], I. Drivas-koulouris[10], A. S. Drobac[157], M. Drozdova[56], D. Du[62a], T. A. du Pree[113], F. Dubinin[37], M. Dubovsky[28a], E. Duchovni[168], G. Duckeck[108], O. A. Ducu[27b], D. Duda[109], A. Dudarev[36], M. D'uffizi[100], L. Duflot[66], M. Dührssen[36], C. Dülsen[170], A. E. Dumitriu[27b], M. Dunford[63a], S. Dungs[49], K. Dunne[47a,47b], A. Duperrin[101], H. Duran Yildiz[3a], M. Düren[58], A. Durglishvili[148b], B. L. Dwyer[114], G. I. Dyckes[17a], M. Dyndal[84a], S. Dysch[100], B. S. Dziedzic[85], Z. O. Earnshaw[145], B. Eckerova[28a], S. Eggebrecht[55], M. G. Eggleston[51], E. Egidio Purcino De Souza[81b], L. F. Ehrke[56], G. Eigen[16], K. Einsweiler[17a], T. Ekelof[160], P. A. Ekman[97], Y. El Ghazali[35b], H. El Jarrari[35e,147], A. El Moussaouy[35a], V. Ellajosyula[160], M. Ellert[160], F. Ellinghaus[170], A. A. Elliot[93], N. Ellis[36], J. Elmsheuser[29], M. Elsing[36], D. Emeliyanov[133], A. Emerman[41], Y. Enari[152], I. Ene[17a], S. Epari[13], J. Erdmann[49,ac], A. Ereditato[19], P. A. Erland[85], M. Errenst[170], M. Escalier[66], C. Escobar[162], E. Etzion[150], G. Evans[129a], H. Evans[67], M. O. Evans[145], A. Ezhilov[37], S. Ezzarqtouni[35a], F. Fabbri[59], L. Fabbri[23a,23b], G. Facini[95], V. Fadeyev[135], R. M. Fakhrutdinov[37], S. Falciano[74a], P. J. Falke[24], S. Falke[36], J. Faltova[132], Y. Fan[14a], Y. Fang[14a,14d], G. Fanourakis[46], M. Fanti[70a,70b], M. Faraj[68a,68b], Z. Farazpay[96], A. Farbin[8], A. Farilla[76a], T. Farooque[106], S. M. Farrington[52], F. Fassi[35e], D. Fassouliotis[9], M. Faucci Giannelli[75a,75b], W. J. Fawcett[32], L. Fayard[66], P. Federicova[130], O. L. Fedin[37,a], G. Fedotov[37], M. Feickert[169], L. Feligioni[101], A. Fell[138], D. E. Fellers[122], C. Feng[62b], M. Feng[14b], Z. Feng[113], M. J. Fenton[159], A. B. Fenyuk[37], L. Ferencz[48], J. Ferrando[48], A. Ferrari[160], P. Ferrari[112,113], R. Ferrari[72a], D. Ferrere[56], C. Ferretti[105], F. Fiedler[99], A. Filipčič[92], E. K. Filmer[1], F. Filthaut[112], M. C. N. Fiolhais[129a,129c,b], L. Fiorini[162], F. Fischer[140], W. C. Fisher[106], T. Fitschen[100], I. Fleck[140], P. Fleischmann[105], T. Flick[170], L. Flores[127], M. Flores[33d], L. R. Flores Castillo[64a], F. M. Follega[77a,77b], N. Fomin[16], J. H. Foo[154], B. C. Forland[67], A. Formica[134], A. C. Forti[100], E. Fortin[101], A. W. Fortman[61], M. G. Foti[17a], L. Fountas[9,j], D. Fournier[66], H. Fox[90], P. Francavilla[73a,73b], S. Francescato[61], S. Franchellucci[56], M. Franchini[23a,23b], S. Franchino[63a], D. Francis[36], L. Franco[112], L. Franconi[19], M. Franklin[61], G. Frattari[26], A. C. Freegard[93], P. M. Freeman[20], W. S. Freund[81b], N. Fritzsche[50], A. Froch[54], D. Froidevaux[36], J. A. Frost[125], Y. Fu[62a], M. Fujimoto[117], E. Fullana Torregrosa[162,*], J. Fuster[162], A. Gabrielli[23a,23b], A. Gabrielli[154], P. Gadow[48], G. Gagliardi[57a,57b], L. G. Gagnon[17a], G. E. Gallardo[125], E. J. Gallas[125], B. J. Gallop[133], R. Gamboa Goni[93], K. K. Gan[118], S. Ganguly[152], J. Gao[62a], Y. Gao[52], F. M. Garay Walls[136a,136b], B. Garcia[29,ah], C. García[162], J. E. García Navarro[162], M. Garcia-Sciveres[17a], R. W. Gardner[39], D. Garg[79], R. B. Garg[142,ao], C. A. Garner[154], V. Garonne[29], S. J. Gasiorowski[137], P. Gaspar[81b], G. Gaudio[72a], V. Gautam[13], P. Gauzzi[74a,74b], I. L. Gavrilenko[37], A. Gavrilyuk[37], C. Gay[163], G. Gaycken[48], E. N. Gazis[10], A. A. Geanta[27b,27e], C. M. Gee[135], J. Geisen[97], C. Gemme[57b], M. H. Genest[60], S. Gentile[74a,74b], S. George[94], W. F. George[20], T. Geralis[46], L. O. Gerlach[55], P. Gessinger-Befurt[36], M. Ghasemi Bostanabad[164], M. Ghneimat[140], K. Ghorbanian[93], A. Ghosal[140], A. Ghosh[159], A. Ghosh[7], B. Giacobbe[23b], S. Giagu[74a,74b], P. Giannetti[73a], A. Giannini[62a], S. M. Gibson[94], M. Gignac[135], D. T. Gil[84b], A. K. Gilbert[84a], B. J. Gilbert[41], D. Gillberg[34], G. Gilles[113], N. E. K. Gillwald[48], L. Ginabat[126], D. M. Gingrich[2,ae], M. P. Giordani[68a,68c], P. F. Giraud[134], G. Giugliarelli[68a,68c], D. Giugni[70a], F. Giuli[36], I. Gkialas[9,j], L. K. Gladilin[37], C. Glasman[98], G. R. Gledhill[122], M. Glisic[122], I. Gnesi[43b,f], Y. Go[29,ah], M. Goblirsch-Kolb[26], B. Gocke[49], D. Godin[107], B. Gokturk[21a], S. Goldfarb[104], T. Golling[56], M. G. D. Gololo[33g], D. Golubkov[37], J. P. Gombas[106], A. Gomes[129a,129b], G. Gomes Da Silva[140], A. J. Gomez Delegido[162], R. Goncalves Gama[55], R. Gonçalo[129a,129c], G. Gonella[122], L. Gonella[20], A. Gongadze[38], F. Gonnella[20], J. L. Gonski[41], R. Y. González Andana[52], S. González de la Hoz[162], S. Gonzalez Fernandez[13], R. Gonzalez Lopez[91], C. Gonzalez Renteria[17a], R. Gonzalez Suarez[160], S. Gonzalez-Sevilla[56], G. R. Gonzalvo Rodriguez[162], L. Goossens[36], N. A. Gorasia[20], P. A. Gorbounov[37], B. Gorini[36], E. Gorini[69a,69b], A. Gorišek[92], A. T. Goshaw[51], M. I. Gostkin[38], C. A. Gottardo[36], M. Gouighri[35b], V. Goumarre[48], A. G. Goussiou[137], N. Govender[33c], C. Goy[4], I. Grabowska-Bold[84a], K. Graham[34], E. Gramstad[124], S. Grancagnolo[18], M. Grandi[145], V. Gratchev[37,*], P. M. Gravila[27f], F. G. Gravili[69a,69b], H. M. Gray[17a], M. Greco[69a,69b], C. Grefe[24], I. M. Gregor[48], P. Grenier[142], C. Grieco[13], A. A. Grillo[135], K. Grimm[31,n], S. Grinstein[13,u], J.-F. Grivaz[66], E. Gross[168], J. Grosse-Knetter[55], C. Grud[105], A. Grummer[111], J. C. Grundy[125], L. Guan[105], W. Guan[169], C. Gubbels[163], J. G. R. Guerrero Rojas[162], G. Guerrieri[68a,68b], F. Guescini[109], R. Gugel[99], J. A. M. Guhit[105], A. Guida[48], T. Guillemin[4], E. Guilloton[166,133], S. Guindon[36], F. Guo[14a,14d], J. Guo[62c], L. Guo[66], Y. Guo[105], R. Gupta[48], S. Gurbuz[24],

S. S. Gurdasani[54], G. Gustavino[36], M. Guth[56], P. Gutierrez[119], L. F. Gutierrez Zagazeta[127], C. Gutschow[95], C. Guyot[134], C. Gwenlan[125], C. B. Gwilliam[91], E. S. Haaland[124], A. Haas[116], M. Habedank[48], C. Haber[17a], H. K. Hadavand[8], A. Hadef[99], S. Hadzic[109], E. H. Haines[95], M. Haleem[165], J. Haley[120], J. J. Hall[138], G. D. Hallewell[101], L. Halser[19], K. Hamano[164], H. Hamdaoui[35e], M. Hamer[24], G. N. Hamity[52], J. Han[62b], K. Han[62a], L. Han[14c], L. Han[62a], S. Han[17a], Y. F. Han[154], K. Hanagaki[82], M. Hance[135], D. A. Hangal[41,ab], H. Hanif[141], M. D. Hank[39], R. Hankache[100], J. B. Hansen[42], J. D. Hansen[42], P. H. Hansen[42], K. Hara[156], D. Harada[56], T. Harenberg[170], S. Harkusha[37], Y. T. Harris[125], N. M. Harrison[118], P. F. Harrison[166], N. M. Hartman[142], N. M. Hartmann[108], Y. Hasegawa[139], A. Hasib[52], S. Haug[19], R. Hauser[106], M. Havranek[131], C. M. Hawkes[20], R. J. Hawkings[36], S. Hayashida[110], D. Hayden[106], C. Hayes[105], R. L. Hayes[163], C. P. Hays[125], J. M. Hays[93], H. S. Hayward[91], F. He[62a], Y. He[153], Y. He[126], M. P. Heath[52], V. Hedberg[97], A. L. Heggelund[124], N. D. Hehir[93], C. Heidegger[54], K. K. Heidegger[54], W. D. Heidorn[80], J. Heilman[34], S. Heim[48], T. Heim[17a], J. G. Heinlein[127], J. J. Heinrich[122,an], L. Heinrich[109,an], J. Hejbal[130], L. Helary[48], A. Held[169], S. Hellesund[124], C. M. Helling[163], S. Hellman[47a,47b], C. Helsens[36], R. C. W. Henderson[90], L. Henkelmann[32], A. M. Henriques Correia[36], H. Herde[97], Y. Hernández Jiménez[144], L. M. Herrmann[24], M. G. Herrmann[108], T. Herrmann[50], G. Herten[54], R. Hertenberger[108], L. Hervas[36], N. P. Hessey[155a], H. Hibi[83], E. Higón-Rodriguez[162], S. J. Hillier[20], I. Hinchliffe[17a], F. Hinterkeuser[24], M. Hirose[123], S. Hirose[156], D. Hirschbuehl[170], T. G. Hitchings[100], B. Hiti[92], J. Hobbs[144], R. Hobincu[27e], N. Hod[168], M. C. Hodgkinson[138], B. H. Hodkinson[32], A. Hoecker[36], J. Hofer[48], D. Hohn[54], T. Holm[24], M. Holzbock[109], L. B. A. H. Hommels[32], B. P. Honan[100], J. Hong[62c], T. M. Hong[128], J. C. Honig[54], A. Hönle[109], B. H. Hooberman[161], W. H. Hopkins[6], Y. Horii[110], S. Hou[147], A. S. Howard[92], J. Howarth[59], J. Hoya[6], M. Hrabovsky[121], A. Hrynevich[48], T. Hryn'ova[4], P. J. Hsu[65], S.-C. Hsu[137], Q. Hu[41], Y. F. Hu[14a,14d,ag], D. P. Huang[95], S. Huang[64b], X. Huang[14c], Y. Huang[62a], Y. Huang[14a], Z. Huang[100], Z. Hubacek[131], M. Huebner[24], F. Huegging[24], T. B. Huffman[125], M. Huhtinen[36], S. K. Huiberts[16], R. Hulsken[103], N. Huseynov[12,a], J. Huston[106], J. Huth[61], R. Hyneman[142], S. Hyrych[28a], G. Iacobucci[56], G. Iakovidis[29], I. Ibragimov[140], L. Iconomidou-Fayard[66], P. Iengo[71a,71b], R. Iguchi[152], T. Iizawa[56], Y. Ikegami[82], A. Ilg[19], N. Ilic[154], H. Imam[35a], T. Ingebretsen Carlson[47a,47b], G. Introzzi[72a,72b], M. Iodice[76a], V. Ippolito[74a,74b], M. Ishino[152], W. Islam[169], C. Issever[18,48], S. Istin[21a,aj], H. Ito[167], J. M. Iturbe Ponce[64a], R. Iuppa[77a,77b], A. Ivina[168], J. M. Izen[45], V. Izzo[71a], P. Jacka[130,131], P. Jackson[1], R. M. Jacobs[48], B. P. Jaeger[141], C. S. Jagfeld[108], G. Jäkel[170], K. Jakobs[54], T. Jakoubek[168], J. Jamieson[59], K. W. Janas[84a], G. Jarlskog[97], A. E. Jaspan[91], M. Javurkova[102], F. Jeanneau[134], L. Jeanty[122], J. Jejelava[148a,aa], P. Jenni[54,g], C. E. Jessiman[34], S. Jézéquel[4], J. Jia[144], X. Jia[61], X. Jia[14a,14d], Z. Jia[14c], Y. Jiang[62a], S. Jiggins[52], J. Jimenez Pena[109], S. Jin[14c], A. Jinaru[27b], O. Jinnouchi[153], P. Johansson[138], K. A. Johns[7], J. W. Johnson[135], D. M. Jones[32], E. Jones[166], P. Jones[32], R. W. L. Jones[90], T. J. Jones[91], R. Joshi[118], J. Jovicevic[15], X. Ju[17a], J. J. Junggeburth[36], T. Junkermann[63a], A. Juste Rozas[13,u], S. Kabana[136e], A. Kaczmarska[85], M. Kado[74a,74b], H. Kagan[118], M. Kagan[142], A. Kahn[41], A. Kahn[127], C. Kahra[99], T. Kaji[167], E. Kajomovitz[149], N. Kakati[168], C. W. Kalderon[29], A. Kamenshchikov[154], S. Kanayama[153], N. J. Kang[135], D. Kar[33g], K. Karava[125], M. J. Kareem[155b], E. Karentzos[54], I. Karkanias[151,e], S. N. Karpov[38], Z. M. Karpova[38], V. Kartvelishvili[90], A. N. Karyukhin[37], E. Kasimi[151,e], C. Kato[62d], J. Katzy[48], S. Kaur[34], K. Kawade[139], K. Kawagoe[88], T. Kawamoto[134], G. Kawamura[55], E. F. Kay[164], F. I. Kaya[157], S. Kazakos[13], V. F. Kazanin[37], Y. Ke[144], J. M. Keaveney[33a], R. Keeler[164], G. V. Kehris[61], J. S. Keller[34], A. S. Kelly[95], D. Kelsey[145], J. J. Kempster[20], K. E. Kennedy[41], P. D. Kennedy[99], O. Kepka[130], B. P. Kerridge[166], S. Kersten[170], B. P. Kerševan[92], S. Keshri[66], L. Keszeghova[28a], S. Ketabchi Haghighat[154], M. Khandoga[126], A. Khanov[120], A. G. Kharlamov[37], T. Kharlamova[37], E. E. Khoda[137], T. J. Khoo[18], G. Khoriauli[165], J. Khubua[148b], Y. A. R. Khwaira[66], M. Kiehn[36], A. Kilgallon[122], D. W. Kim[47a,47b], E. Kim[153], Y. K. Kim[39], N. Kimura[95], A. Kirchhoff[55], D. Kirchmeier[50], C. Kirfel[24], J. Kirk[133], A. E. Kiryunin[109], T. Kishimoto[152], D. P. Kisliuk[154], C. Kitsaki[10], O. Kivernyk[24], M. Klassen[63a], C. Klein[34], L. Klein[165], M. H. Klein[105], M. Klein[91], S. B. Klein[56], U. Klein[91], P. Klimek[36], A. Klimentov[29], F. Klimpel[109], T. Klioutchnikova[36], P. Kluit[113], S. Kluth[109], E. Kneringer[78], T. M. Knight[154], A. Knue[54], D. Kobayashi[88], R. Kobayashi[86], M. Kocian[142], P. Kodyš[132], D. M. Koeck[145], P. T. Koenig[24], T. Koffas[34], M. Kolb[134], I. Koletsou[4], T. Komarek[121], K. Köneke[54], A. X. Y. Kong[1], T. Kono[117], N. Konstantinidis[95], B. Konya[97], R. Kopeliansky[67], S. Koperny[84a], K. Korcyl[85], K. Kordas[151,e], G. Koren[150], A. Korn[95], S. Korn[55], I. Korolkov[13], N. Korotkova[37], B. Kortman[113], O. Kortner[109], S. Kortner[109], W. H. Kostecka[114], V. V. Kostyukhin[140], A. Kotsokechagia[134], A. Kotwal[51], A. Koulouris[36], A. Kourkoumeli-Charalampidi[72a,72b], C. Kourkoumelis[9], E. Kourlitis[6],

O. Kovanda[145], R. Kowalewski[164], W. Kozanecki[134], A. S. Kozhin[37], V. A. Kramarenko[37], G. Kramberger[92], P. Kramer[99], M. W. Krasny[126], A. Krasznahorkay[36], J. A. Kremer[99], T. Kresse[50], J. Kretzschmar[91], K. Kreul[18], P. Krieger[154], S. Krishnamurthy[102], M. Krivos[132], K. Krizka[17a], K. Kroeninger[49], H. Kroha[109], J. Kroll[130], J. Kroll[127], K. S. Krowpman[106], U. Kruchonak[38], H. Krüger[24], N. Krumnack[80], M. C. Kruse[51], J. A. Krzysiak[85], O. Kuchinskaia[37], S. Kuday[3a], D. Kuechler[48], J. T. Kuechler[48], S. Kuehn[36], T. Kuhl[48], V. Kukhtin[38], Y. Kulchitsky[37,a], S. Kuleshov[136b,136d], M. Kumar[33g], N. Kumari[101], A. Kupco[130], T. Kupfer[49], A. Kupich[37], O. Kuprash[54], H. Kurashige[83], L. L. Kurchaninov[155a], Y. A. Kurochkin[37], A. Kurova[37], M. Kuze[153], A. K. Kvam[102], J. Kvita[121], T. Kwan[103], K. W. Kwok[64a], N. G. Kyriacou[105], L. A. O. Laatu[101], C. Lacasta[162], F. Lacava[74a,74b], H. Lacker[18], D. Lacour[126], N. N. Lad[95], E. Ladygin[38], B. Laforge[126], T. Lagouri[136e], S. Lai[55], I. K. Lakomiec[84a], N. Lalloue[60], J. E. Lambert[119], S. Lammers[67], W. Lampl[7], C. Lampoudis[151,e], A. N. Lancaster[114], E. Lançon[29], U. Landgraf[54], M. P. J. Landon[93], V. S. Lang[54], R. J. Langenberg[102], A. J. Lankford[159], F. Lanni[36], K. Lantzsch[24], A. Lanza[72a], A. Lapertosa[57b,57a], J. F. Laporte[134], T. Lari[70a], F. Lasagni Manghi[23b], M. Lassnig[36], V. Latonova[130], T. S. Lau[64a], A. Laudrain[99], A. Laurier[34], S. D. Lawlor[94], Z. Lawrence[100], M. Lazzaroni[70a,70b], B. Le[100], B. Leban[92], A. Lebedev[80], M. LeBlanc[36], T. LeCompte[6], F. Ledroit-Guillon[60], A. C. A. Lee[95], G. R. Lee[16], L. Lee[61], S. C. Lee[147], S. Lee[47a,47b], T. F. Lee[91], L. L. Leeuw[33c], H. P. Lefebvre[94], M. Lefebvre[164], C. Leggett[17a], K. Lehmann[141], G. Lehmann Miotto[36], M. Leigh[56], W. A. Leight[102], A. Leisos[151,t], M. A. L. Leite[81c], C. E. Leitgeb[48], R. Leitner[132], K. J. C. Leney[44], T. Lenz[24], S. Leone[73a], C. Leonidopoulos[52], A. Leopold[143], C. Leroy[107], R. Les[106], C. G. Lester[32], M. Levchenko[37], J. Levêque[4], D. Levin[105], L. J. Levinson[168], M. P. Lewicki[85], D. J. Lewis[4], A. Li[5], B. Li[62b], C. Li[62a], C-Q. Li[62c], H. Li[62a], H. Li[62b], H. Li[14c], H. Li[62b], J. Li[62c], K. Li[137], L. Li[62c], M. Li[14a,14d], Q. Y. Li[62a], S. Li[14a,14d], S. Li[62d,62c,d], T. Li[62b], X. Li[103], Z. Li[62b], Z. Li[125], Z. Li[103], Z. Li[91], Z. Li[14a,14d], Z. Liang[14a], M. Liberatore[48], B. Liberti[75a], K. Lie[64c], J. Lieber Marin[81b], K. Lin[106], R. A. Linck[67], R. E. Lindley[7], J. H. Lindon[2], A. Linss[48], E. Lipeles[127], A. Lipniacka[16], A. Lister[163], J. D. Little[4], B. Liu[14a], B. X. Liu[141], D. Liu[62d,62c], J. B. Liu[62a], J. K. K. Liu[32], K. Liu[62d,62c], M. Liu[62a], M. Y. Liu[62a], P. Liu[14a], Q. Liu[62d,137,62c], X. Liu[62a], Y. Liu[14c,14d], Y. L. Liu[105], Y. W. Liu[62a], M. Livan[72a,72b], J. Llorente Merino[141], S. L. Lloyd[93], E. M. Lobodzinska[48], P. Loch[7], S. Loffredo[75a,75b], T. Lohse[18], K. Lohwasser[138], M. Lokajicek[130], J. D. Long[161], I. Longarini[159], L. Longo[69a,69b], R. Longo[161], I. Lopez Paz[36], A. Lopez Solis[48], J. Lorenz[108], N. Lorenzo Martinez[4], A. M. Lory[108], X. Lou[47a,47b], X. Lou[14a,14d], A. Lounis[66], J. Love[6], P. A. Love[90], J. J. Lozano Bahilo[162], G. Lu[14a,14d], M. Lu[79], S. Lu[127], Y. J. Lu[65], H. J. Lubatti[137], C. Luci[74a,74b], F. L. Lucio Alves[14c], A. Lucotte[60], F. Luehring[67], I. Luise[144], O. Lukianchuk[66], O. Lundberg[143], B. Lund-Jensen[143], N. A. Luongo[122], M. S. Lutz[150], D. Lynn[29], H. Lyons[91], R. Lysak[130], E. Lytken[97], F. Lyu[14a], V. Lyubushkin[38], T. Lyubushkina[38], H. Ma[29], L. L. Ma[62b], Y. Ma[95], D. M. Mac Donell[164], G. Maccarrone[53], J. C. MacDonald[138], R. Madar[40], W. F. Mader[50], J. Maeda[83], T. Maeno[29], M. Maerker[50], H. Maguire[138], D. J. Mahon[41], A. Maio[129a,129b,129d], K. Maj[84a], O. Majersky[28a], S. Majewski[122], N. Makovec[66], V. Maksimovic[15], B. Malaescu[126], Pa. Malecki[85], V. P. Maleev[37], F. Malek[60], D. Malito[43a,43b], U. Mallik[79], C. Malone[32], S. Maltezos[10], S. Malyukov[38], J. Mamuzic[13], G. Mancini[53], G. Manco[72a,72b], J. P. Mandalia[93], I. Mandić[92], L. Manhaes de Andrade Filho[81a], I. M. Maniatis[151,e], M. Manisha[134], J. Manjarres Ramos[50], D. C. Mankad[168], A. Mann[108], B. Mansoulie[134], S. Manzoni[36], A. Marantis[151,t], G. Marchiori[5], M. Marcisovsky[130], C. Marcon[70a,70b], M. Marinescu[20], M. Marjanovic[119], E. J. Marshall[90], Z. Marshall[17a], S. Marti-Garcia[162], T. A. Martin[166], V. J. Martin[52], B. Martin dit Latour[16], L. Martinelli[74a,74b], M. Martinez[13,u], P. Martinez Agullo[162], V. I. Martinez Outschoorn[102], P. Martinez Suarez[13], S. Martin-Haugh[133], V. S. Martoiu[27b], A. C. Martyniuk[95], A. Marzin[36], S. R. Maschek[109], D. Mascione[77a,77b], L. Masetti[99], T. Mashimo[152], J. Masik[100], A. L. Maslennikov[37], L. Massa[23b], P. Massarotti[71a,71b], P. Mastrandrea[73a,73b], A. Mastroberardino[43a,43b], T. Masubuchi[152], T. Mathisen[160], N. Matsuzawa[152], J. Maurer[27b], B. Maček[92], D. A. Maximov[37], R. Mazini[147], I. Maznas[151,e], M. Mazza[106], S. M. Mazza[135], C. Mc Ginn[29], J. P. Mc Gowan[103], S. P. Mc Kee[105], W. P. McCormack[17a], E. F. McDonald[104], A. E. McDougall[113], J. A. Mcfayden[145], G. Mchedlidze[148b], R. P. Mckenzie[33g], T. C. Mclachlan[48], D. J. Mclaughlin[95], K. D. McLean[164], S. J. McMahon[133], P. C. McNamara[104], C. M. Mcpartland[91], R. A. McPherson[164,x], T. Megy[40], S. Mehlhase[108], A. Mehta[91], B. Meirose[45], D. Melini[149], B. R. Mellado Garcia[33g], A. H. Melo[55], F. Meloni[48], E. D. Mendes Gouveia[129a], A. M. Mendes Jacques Da Costa[20], H. Y. Meng[154], L. Meng[90], S. Menke[109], M. Mentink[36], E. Meoni[43a,43b], C. Merlassino[125], L. Merola[71a,71b], C. Meroni[70a],

G. Merz[105], O. Meshkov[37], J. Metcalfe[6], A. S. Mete[6], C. Meyer[67], J-P. Meyer[134], M. Michetti[18], R. P. Middleton[133], L. Mijović[52], G. Mikenberg[168], M. Mikestikova[130], M. Mikuž[92], H. Mildner[138], A. Milic[36], C. D. Milke[44], D. W. Miller[39], L. S. Miller[34], A. Milov[168], D. A. Milstead[47a,47b], T. Min[14c], A. A. Minaenko[37], I. A. Minashvili[148b], L. Mince[59], A. I. Mincer[116], B. Mindur[84a], M. Mineev[38], Y. Mino[86], L. M. Mir[13], M. Miralles Lopez[162], M. Mironova[125], M. C. Missio[112], T. Mitani[167], A. Mitra[166], V. A. Mitsou[162], O. Miu[154], P. S. Miyagawa[93], Y. Miyazaki[88], A. Mizukami[82], J. U. Mjörnmark[97], T. Mkrtchyan[63a], T. Mlinarevic[95], M. Mlynarikova[36], T. Moa[47a,47b], S. Mobius[55], K. Mochizuki[107], P. Moder[48], P. Mogg[108], A. F. Mohammed[14a,14d], S. Mohapatra[41], G. Mokgatitswane[33g], B. Mondal[140], S. Mondal[131], K. Mönig[48], E. Monnier[101], L. Monsonis Romero[162], J. Montejo Berlingen[36], M. Montella[118], F. Monticelli[89], N. Morange[66], A. L. Moreira De Carvalho[129a], M. Moreno Llácer[162], C. Moreno Martinez[56], P. Morettini[57b], S. Morgenstern[166], M. Morii[61], M. Morinaga[152], A. K. Morley[36], F. Morodei[74a,74b], L. Morvaj[36], P. Moschovakos[36], B. Moser[36], M. Mosidze[148b], T. Moskalets[54], P. Moskvitina[112], J. Moss[31,o], E. J. W. Moyse[102], O. Mtintsilana[33g], S. Muanza[101], J. Mueller[128], D. Muenstermann[90], R. Müller[19], G. A. Mullier[160], J. J. Mullin[127], D. P. Mungo[154], J. L. Munoz Martinez[13], D. Munoz Perez[162], F. J. Munoz Sanchez[100], M. Murin[100], W. J. Murray[166,133], A. Murrone[70a,70b], J. M. Muse[119], M. Muškinja[17a], C. Mwewa[29], A. G. Myagkov[37,a], A. J. Myers[8], A. A. Myers[128], G. Myers[67], M. Myska[131], B. P. Nachman[17a], O. Nackenhorst[49], A. Nag[50], K. Nagai[125], K. Nagano[82], J. L. Nagle[29,ah], E. Nagy[101], A. M. Nairz[36], Y. Nakahama[82], K. Nakamura[82], H. Nanjo[123], R. Narayan[44], E. A. Narayanan[111], I. Naryshkin[37], M. Naseri[34], C. Nass[24], G. Navarro[22a], J. Navarro-Gonzalez[162], R. Nayak[150], A. Nayaz[18], P. Y. Nechaeva[37], F. Nechansky[48], L. Nedic[125], T. J. Neep[20], A. Negri[72a,72b], M. Negrini[23b], C. Nellist[112], C. Nelson[103], K. Nelson[105], S. Nemecek[130], M. Nessi[36,h], M. S. Neubauer[161], F. Neuhaus[99], J. Neundorf[48], R. Newhouse[163], P. R. Newman[20], C. W. Ng[128], Y. S. Ng[18], Y. W. Y. Ng[48], B. Ngair[35e], H. D. N. Nguyen[107], R. B. Nickerson[125], R. Nicolaidou[134], J. Nielsen[135], M. Niemeyer[55], N. Nikiforou[36], V. Nikolaenko[37,a], I. Nikolic-Audit[126], K. Nikolopoulos[20], P. Nilsson[29], I. Ninca[48], H. R. Nindhito[56], A. Nisati[74a], N. Nishu[2], R. Nisius[109], J-E. Nitschke[50], E. K. Nkadimeng[33g], S. J. Noacco Rosende[89], T. Nobe[152], D. L. Noel[32], Y. Noguchi[86], T. Nommensen[146], M. A. Nomura[29], M. B. Norfolk[138], R. R. B. Norisam[95], B. J. Norman[34], J. Novak[92], T. Novak[48], O. Novgorodova[50], L. Novotny[131], R. Novotny[111], L. Nozka[121], K. Ntekas[159], N. M. J. Nunes De Moura Junior[81b], E. Nurse[95], F. G. Oakham[34,ae], J. Ocariz[126], A. Ochi[83], I. Ochoa[129a], S. Oerdek[160], A. Ogrodnik[84a], A. Oh[100], C. C. Ohm[143], H. Oide[82], R. Oishi[152], M. L. Ojeda[48], Y. Okazaki[86], M. W. O'Keefe[91], Y. Okumura[152], A. Olariu[27b], L. F. Oleiro Seabra[129a], S. A. Olivares Pino[136e], D. Oliveira Damazio[29], D. Oliveira Goncalves[81a], J. L. Oliver[159], M. J. R. Olsson[159], A. Olszewski[85], J. Olszowska[85,*], Ö. O. Öncel[54], D. C. O'Neil[141], A. P. O'Neill[19], A. Onofre[129a,129e], P. U. E. Onyisi[11], M. J. Oreglia[39], G. E. Orellana[89], D. Orestano[76a,76b], N. Orlando[13], R. S. Orr[154], V. O'Shea[59], R. Ospanov[62a], G. Otero y Garzon[30], H. Otono[88], P. S. Ott[63a], G. J. Ottino[17a], M. Ouchrif[35d], J. Ouellette[29,ah], F. Ould-Saada[124], M. Owen[59], R. E. Owen[133], K. Y. Oyulmaz[21a], V. E. Ozcan[21a], N. Ozturk[8], S. Ozturk[21d], J. Pacalt[121], H. A. Pacey[32], K. Pachal[51], A. Pacheco Pages[13], C. Padilla Aranda[13], G. Padovano[74a,74b], S. Pagan Griso[17a], G. Palacino[67], A. Palazzo[69a,69b], S. Palestini[36], M. Palka[84b], J. Pan[171], T. Pan[64a], D. K. Panchal[11], C. E. Pandini[113], J. G. Panduro Vazquez[94], H. Pang[14b], P. Pani[48], G. Panizzo[68a,68c], L. Paolozzi[56], C. Papadatos[107], S. Parajuli[44], A. Paramonov[6], C. Paraskevopoulos[10], D. Paredes Hernandez[64b], T. H. Park[154], M. A. Parker[32], F. Parodi[57b,57a], E. W. Parrish[114], V. A. Parrish[52], J. A. Parsons[41], U. Parzefall[54], B. Pascual Dias[107], L. Pascual Dominguez[150], V. R. Pascuzzi[17a], F. Pasquali[113], E. Pasqualucci[74a], S. Passaggio[57b], F. Pastore[94], P. Pasuwan[47a,47b], P. Patel[85], J. R. Pater[100], T. Pauly[36], J. Pearkes[142], M. Pedersen[124], R. Pedro[129a], S. V. Peleganchuk[37], O. Penc[36], E. A. Pender[52], C. Peng[64b], H. Peng[62a], K. E. Penski[108], M. Penzin[37], B. S. Peralva[81d,81d], A. P. Pereira Peixoto[60], L. Pereira Sanchez[47a,47b], D. V. Perepelitsa[29,ah], E. Perez Codina[155a], M. Perganti[10], L. Perini[70a,70b,*], H. Pernegger[36], S. Perrella[36], A. Perrevoort[112], O. Perrin[40], K. Peters[48], R. F. Y. Peters[100], B. A. Petersen[36], T. C. Petersen[42], E. Petit[101], V. Petousis[131], C. Petridou[151,e], A. Petrukhin[140], M. Pettee[17a], N. E. Pettersson[36], A. Petukhov[37], K. Petukhova[132], A. Peyaud[134], R. Pezoa[136f], L. Pezzotti[36], G. Pezzullo[171], T. M. Pham[169], T. Pham[104], P. W. Phillips[133], M. W. Phipps[161], G. Piacquadio[144], E. Pianori[17a], F. Piazza[70a,70b], R. Piegaia[30], D. Pietreanu[27b], A. D. Pilkington[100], M. Pinamonti[68a,68c], J. L. Pinfold[2], B. C. Pinheiro Pereira[129a], C. Pitman Donaldson[95], D. A. Pizzi[34], L. Pizzimento[75a,75b], A. Pizzini[113], M.-A. Pleier[29], V. Plesanovs[54], V. Pleskot[132], E. Plotnikova[38], G. Poddar[4], R. Poettgen[97], L. Poggioli[126], I. Pogrebnyak[106], D. Pohl[24], I. Pokharel[55], S. Polacek[132], G. Polesello[72a], A. Poley[141,155a],

R. Polifka[131], A. Polini[23b], C. S. Pollard[166], Z. B. Pollock[118], V. Polychronakos[29], E. Pompa Pacchi[74a,74b], D. Ponomarenko[37], L. Pontecorvo[36], S. Popa[27a], G. A. Popeneciu[27d], D. M. Portillo Quintero[155a], S. Pospisil[131], P. Postolache[27c], K. Potamianos[125], I. N. Potrap[38], C. J. Potter[32], H. Potti[1], T. Poulsen[48], J. Poveda[162], M. E. Pozo Astigarraga[36], A. Prades Ibanez[162], M. M. Prapa[46], J. Pretel[54], D. Price[100], M. Primavera[69a], M. A. Principe Martin[98], R. Privara[121], M. L. Proffitt[137], N. Proklova[127], K. Prokofiev[64c], G. Proto[75a,75b], S. Protopopescu[29], J. Proudfoot[6], M. Przybycien[84a], J. E. Puddefoot[138], D. Pudzha[37], P. Puzo[66], D. Pyatiizbyantseva[37], J. Qian[105], D. Qichen[100], Y. Qin[100], T. Qiu[93], A. Quadt[55], M. Queitsch-Maitland[100], G. Quetant[56], G. Rabanal Bolanos[61], D. Rafanoharana[54], F. Ragusa[70a,70b], J. L. Rainbolt[39], J. A. Raine[56], S. Rajagopalan[29], E. Ramakoti[37], K. Ran[48,14d], N. P. Rapheeha[33g], V. Raskina[126], D. F. Rassloff[63a], S. Rave[99], B. Ravina[55], I. Ravinovich[168], M. Raymond[36], A. L. Read[124], N. P. Readioff[138], D. M. Rebuzzi[72a,72b], G. Redlinger[29], K. Reeves[45], J. A. Reidelsturz[170], D. Reikher[150], A. Rej[140], C. Rembser[36], A. Renardi[48], M. Renda[27b], M. B. Rendel[109], F. Renner[48], A. G. Rennie[59], S. Resconi[70a], M. Ressegotti[57b,57a], E. D. Resseguie[17a], S. Rettie[36], J. G. Reyes Rivera[106], B. Reynolds[118], E. Reynolds[17a], M. Rezaei Estabragh[170], O. L. Rezanova[37], P. Reznicek[132], E. Ricci[77a,77b], R. Richter[109], S. Richter[47a,47b], E. Richter-Was[84b], M. Ridel[126], S. Ridouani[35d], P. Rieck[116], P. Riedler[36], M. Rijssenbeek[144], A. Rimoldi[72a,72b], M. Rimoldi[48], L. Rinaldi[23a,23b], T. T. Rinn[29], M. P. Rinnagel[108], G. Ripellino[143], I. Riu[13], P. Rivadeneira[48], J. C. Rivera Vergara[164], F. Rizatdinova[120], E. Rizvi[93], C. Rizzi[56], B. A. Roberts[166], B. R. Roberts[17a], S. H. Robertson[103,x], M. Robin[48], D. Robinson[32], C. M. Robles Gajardo[136f], M. Robles Manzano[99], A. Robson[59], A. Rocchi[75a,75b], C. Roda[73a,73b], S. Rodriguez Bosca[63a], Y. Rodriguez Garcia[22a], A. Rodriguez Rodriguez[54], A. M. Rodríguez Vera[155b], S. Roe[36], J. T. Roemer[159], A. R. Roepe-Gier[119], J. Roggel[170], O. Røhne[124], R. A. Rojas[102], B. Roland[54], C. P. A. Roland[67], J. Roloff[29], A. Romaniouk[37], E. Romano[72a,72b], M. Romano[23b], A. C. Romero Hernandez[161], N. Rompotis[91], L. Roos[126], S. Rosati[74a], B. J. Rosser[39], E. Rossi[4], E. Rossi[71a,71b], L. P. Rossi[57b], L. Rossini[48], R. Rosten[118], M. Rotaru[27b], B. Rottler[54], D. Rousseau[66], D. Rousso[32], G. Rovelli[72a,72b], A. Roy[161], A. Rozanov[101], Y. Rozen[149], X. Ruan[33g], A. Rubio Jimenez[162], A. J. Ruby[91], V. H. Ruelas Rivera[18], T. A. Ruggeri[1], F. Rühr[54], A. Ruiz-Martinez[162], A. Rummler[36], Z. Rurikova[54], N. A. Rusakovich[38], H. L. Russell[164], J. P. Rutherfoord[7], K. Rybacki[90], M. Rybar[132], E. B. Rye[124], A. Ryzhov[37], J. A. Sabater Iglesias[56], P. Sabatini[162], L. Sabetta[74a,74b], H. F-W. Sadrozinski[135], F. Safai Tehrani[74a], B. Safarzadeh Samani[145], M. Safdari[142], S. Saha[103], M. Sahinsoy[109], M. Saimpert[134], M. Saito[152], T. Saito[152], D. Salamani[36], G. Salamanna[76a,76b], A. Salnikov[142], J. Salt[162], A. Salvador Salas[13], D. Salvatore[43a,43b], F. Salvatore[145], A. Salzburger[36], D. Sammel[54], D. Sampsonidis[151,e], D. Sampsonidou[62d,62c], J. Sánchez[162], A. Sanchez Pineda[4], V. Sanchez Sebastian[162], H. Sandaker[124], C. O. Sander[48], J. A. Sandesara[102], M. Sandhoff[170], C. Sandoval[22b], D. P. C. Sankey[133], A. Sansoni[53], L. Santi[74a,74b], C. Santoni[40], H. Santos[129a,129b], S. N. Santpur[17a], A. Santra[168], K. A. Saoucha[138], J. G. Saraiva[129a,129d], J. Sardain[7], O. Sasaki[82], K. Sato[156], C. Sauer[63b], F. Sauerburger[54], E. Sauvan[4], P. Savard[154,ae], R. Sawada[152], C. Sawyer[133], L. Sawyer[96], I. Sayago Galvan[162], C. Sbarra[23b], A. Sbrizzi[23a,23b], T. Scanlon[95], J. Schaarschmidt[137], P. Schacht[109], D. Schaefer[39], U. Schäfer[99], A. C. Schaffer[66,44], D. Schaile[108], R. D. Schamberger[144], E. Schanet[108], C. Scharf[18], M. M. Schefer[19], V. A. Schegelsky[37], D. Scheirich[132], F. Schenck[18], M. Schernau[159], C. Scheulen[55], C. Schiavi[57b,57a], Z. M. Schillaci[26], E. J. Schioppa[69a,69b], M. Schioppa[43a,43b], B. Schlag[99], K. E. Schleicher[54], S. Schlenker[36], J. Schmeing[170], M. A. Schmidt[170], K. Schmieden[99], C. Schmitt[99], S. Schmitt[48], L. Schoeffel[134], A. Schoening[63b], P. G. Scholer[54], E. Schopf[125], M. Schott[99], J. Schovancova[36], S. Schramm[56], F. Schroeder[170], H-C. Schultz-Coulon[63a], M. Schumacher[54], B. A. Schumm[135], Ph. Schune[134], A. Schwartzman[142], T. A. Schwarz[105], Ph. Schwemling[134], R. Schwienhorst[106], A. Sciandra[135], G. Sciolla[26], F. Scuri[73a], F. Scutti[104], C. D. Sebastiani[91], K. Sedlaczek[49], P. Seema[18], S. C. Seidel[111], A. Seiden[135], B. D. Seidlitz[41], C. Seitz[48], J. M. Seixas[81b], G. Sekhniaidze[71a], S. J. Sekula[44], L. Selem[4], N. Semprini-Cesari[23a,23b], S. Sen[51], D. Sengupta[56], V. Senthilkumar[162], L. Serin[66], L. Serkin[68a,68b], M. Sessa[76a,76b], H. Severini[119], S. Sevova[142], F. Sforza[57b,57a], A. Sfyrla[56], E. Shabalina[55], R. Shaheen[143], J. D. Shahinian[127], D. Shaked Renous[168], L. Y. Shan[14a], M. Shapiro[17a], A. Sharma[36], A. S. Sharma[163], P. Sharma[79], S. Sharma[48], P. B. Shatalov[37], K. Shaw[145], S. M. Shaw[100], Q. Shen[62c,5], P. Sherwood[95], L. Shi[95], C. O. Shimmin[171], Y. Shimogama[167], J. D. Shinner[94], I. P. J. Shipsey[125], S. Shirabe[60], M. Shiyakova[38,ap], J. Shlomi[168], M. J. Shochet[39], J. Shojaii[104], D. R. Shope[124], S. Shrestha[118,ai], E. M. Shrif[33g], M. J. Shroff[164], P. Sicho[130], A. M. Sickles[161], E. Sideras Haddad[33g], A. Sidoti[23b], F. Siegert[50], Dj. Sijacki[15], R. Sikora[84a], F. Sili[89], J. M. Silva[20],

M. V. Silva Oliveira[36], S. B. Silverstein[47a], S. Simion[66], R. Simoniello[36], E. L. Simpson[59], L. R. Simpson[105], N. D. Simpson[97], S. Simsek[21d], S. Sindhu[55], P. Sinervo[154], S. Singh[141], S. Singh[154], S. Sinha[48], S. Sinha[33g], M. Sioli[23a,23b], I. Siral[36], S. Yu. Sivoklokov[37,*], J. Sjölin[47a,47b], A. Skaf[55], E. Skorda[97], P. Skubic[119], M. Slawinska[85], V. Smakhtin[168], B. H. Smart[133], J. Smiesko[36], S.Yu. Smirnov[37], Y. Smirnov[37], L. N. Smirnova[37,a], O. Smirnova[97], A. C. Smith[41], E. A. Smith[39], H. A. Smith[125], J. L. Smith[91], R. Smith[142], M. Smizanska[90], K. Smolek[131], A. Smykiewicz[85], A. A. Snesarev[37], H. L. Snoek[113], S. Snyder[29], R. Sobie[164,x], A. Soffer[150], C. A. Solans Sanchez[36], E. Yu. Soldatov[37], U. Soldevila[162], A. A. Solodkov[37], S. Solomon[54], A. Soloshenko[38], K. Solovieva[54], O. V. Solovyanov[40], V. Solovyev[37], P. Sommer[36], A. Sonay[13], W. Y. Song[155b], A. Sopczak[131], A. L. Sopio[95], F. Sopkova[28b], V. Sothilingam[63a], S. Sottocornola[72a,72b], R. Soualah[115b], Z. Soumaimi[35e], D. South[48], S. Spagnolo[69a,69b], M. Spalla[109], F. Spanò[94], D. Sperlich[54], G. Spigo[36], M. Spina[145], S. Spinali[90], D. P. Spiteri[59], M. Spousta[132], E. J. Staats[34], A. Stabile[70a,70b], R. Stamen[63a], M. Stamenkovic[113], A. Stampekis[20], M. Standke[24], E. Stanecka[85], M. V. Stange[50], B. Stanislaus[17a], M. M. Stanitzki[48], M. Stankaityte[125], B. Stapf[48], E. A. Starchenko[37], G. H. Stark[135], J. Stark[101,am], D. M. Starko[155b], P. Staroba[130], P. Starovoitov[63a], S. Stärz[103], R. Staszewski[85], G. Stavropoulos[46], J. Steentoft[160], P. Steinberg[29], A. L. Steinhebel[122], B. Stelzer[141,155a], H. J. Stelzer[128], O. Stelzer-Chilton[155a], H. Stenzel[58], T. J. Stevenson[145], G. A. Stewart[36], M. C. Stockton[36], G. Stoicea[27b], M. Stolarski[129a], S. Stonjek[109], A. Straessner[50], J. Strandberg[143], S. Strandberg[47a,47b], M. Strauss[119], T. Strebler[101], P. Strizenec[28b], R. Ströhmer[165], D. M. Strom[122], L. R. Strom[48], R. Stroynowski[44], A. Strubig[47a,47b], S. A. Stucci[29], B. Stugu[16], J. Stupak[119], N. A. Styles[48], D. Su[142], S. Su[62a], W. Su[62d,137,62c], X. Su[62a,66], K. Sugizaki[152], V. V. Sulin[37], M. J. Sullivan[91], D. M. S. Sultan[77a,77b], L. Sultanaliyeva[37], S. Sultansoy[3b], T. Sumida[86], S. Sun[105], S. Sun[169], O. Sunneborn Gudnadottir[160], M. R. Sutton[145], M. Svatos[130], M. Swiatlowski[155a], T. Swirski[165], I. Sykora[28a], M. Sykora[132], T. Sykora[132], D. Ta[99], K. Tackmann[48,v], A. Taffard[159], R. Tafirout[155a], J. S. Tafoya Vargas[66], R. H. M. Taibah[126], R. Takashima[87], K. Takeda[83], E. P. Takeva[52], Y. Takubo[82], M. Talby[101], A. A. Talyshev[37], K. C. Tam[64b], N. M. Tamir[150], A. Tanaka[152], J. Tanaka[152], R. Tanaka[66], M. Tanasini[57b,57a], J. Tang[62c], Z. Tao[163], S. Tapia Araya[136f], S. Tapprogge[99], A. Tarek Abouelfadl Mohamed[106], S. Tarem[149], K. Tariq[62b], G. Tarna[101,27b], G. F. Tartarelli[70a], P. Tas[132], M. Tasevsky[130], E. Tassi[43a,43b], A. C. Tate[161], G. Tateno[152], Y. Tayalati[35e,w], G. N. Taylor[104], W. Taylor[155b], H. Teagle[91], A. S. Tee[169], R. Teixeira De Lima[142], P. Teixeira-Dias[94], J. J. Teoh[154], K. Terashi[152], J. Terron[98], S. Terzo[13], M. Testa[53], R. J. Teuscher[154,x], A. Thaler[78], O. Theiner[56], N. Themistokleous[52], T. Theveneaux-Pelzer[18], O. Thielmann[170], D. W. Thomas[94], J. P. Thomas[20], E. A. Thompson[48], P. D. Thompson[20], E. Thomson[127], E. J. Thorpe[93], Y. Tian[55], V. Tikhomirov[37,a], Yu.A. Tikhonov[37], S. Timoshenko[37], E. X. L. Ting[1], P. Tipton[171], S. Tisserant[101], S. H. Tlou[33g], A. Tnourji[40], K. Todome[23a,23b], S. Todorova-Nova[132], S. Todt[50], M. Togawa[82], J. Tojo[88], S. Tokár[28a], K. Tokushuku[82], R. Tombs[32], M. Tomoto[82,110], L. Tompkins[142,ao], K. W. Topolnicki[84b], P. Tornambe[102], E. Torrence[122], H. Torres[50], E. Torró Pastor[162], M. Toscani[30], C. Tosciri[39], M. Tost[11], D. R. Tovey[138], A. Traeet[16], I. S. Trandafir[27b], T. Trefzger[165], A. Tricoli[29], I. M. Trigger[155a], S. Trincaz-Duvoid[126], D. A. Trischuk[26], B. Trocmé[60], A. Trofymov[66], C. Troncon[70a], L. Truong[33c], M. Trzebinski[85], A. Trzupek[85], F. Tsai[144], M. Tsai[105], A. Tsiamis[151,e], P. V. Tsiareshka[37], S. Tsigaridas[155a], A. Tsirigotis[151,t], V. Tsiskaridze[144], E. G. Tskhadadze[148a], M. Tsopoulou[151,e], Y. Tsujikawa[86], I. I. Tsukerman[37], V. Tsulaia[17a], S. Tsuno[82], O. Tsur[149], D. Tsybychev[144], Y. Tu[64b], A. Tudorache[27b], V. Tudorache[27b], A. N. Tuna[36], S. Turchikhin[38], I. Turk Cakir[3a], R. Turra[70a], T. Turtuvshin[38,y], P. M. Tuts[41], S. Tzamarias[151,e], P. Tzanis[10], E. Tzovara[99], K. Uchida[152], F. Ukegawa[156], P. A. Ulloa Poblete[136c], E. N. Umaka[29], G. Unal[36], M. Unal[11], A. Undrus[29], G. Unel[159], J. Urban[28b], P. Urquijo[104], G. Usai[8], R. Ushioda[153], M. Usman[107], Z. Uysal[21b], L. Vacavant[101], V. Vacek[131], B. Vachon[103], K. O. H. Vadla[124], T. Vafeiadis[36], A. Vaitkus[95], C. Valderanis[108], E. Valdes Santurio[47a,47b], M. Valente[155a], S. Valentinetti[23a,23b], A. Valero[162], A. Vallier[101,am], J. A. Valls Ferrer[162], T. R. Van Daalen[137], P. Van Gemmeren[6], M. Van Rijnbach[36,124], S. Van Stroud[95], I. Van Vulpen[113], M. Vanadia[75a,75b], W. Vandelli[36], M. Vandenbroucke[134], E. R. Vandewall[120], D. Vannicola[150], L. Vannoli[57b,57a], R. Vari[74a], E. W. Varnes[7], C. Varni[17a], T. Varol[147], D. Varouchas[66], L. Varriale[162], K. E. Varvell[146], M. E. Vasile[27b], L. Vaslin[40], G. A. Vasquez[164], F. Vazeille[40], T. Vazquez Schroeder[36], J. Veatch[31], V. Vecchio[100], M. J. Veen[102], I. Veliscek[125], L. M. Veloce[154], F. Veloso[129a,129c], S. Veneziano[74a], A. Ventura[69a,69b], A. Verbytskyi[109], M. Verducci[73a,73b], C. Vergis[24], M. Verissimo De Araujo[81b], W. Verkerke[113], J. C. Vermeulen[113], C. Vernieri[142], P. J. Verschuuren[94], M. Vessella[102], M. C. Vetterli[141,ae], A. Vgenopoulos[151,e],

N. Viaux Maira[136f], T. Vickey[138], O. E. Vickey Boeriu[138], G. H. A. Viehhauser[125], L. Vigani[63b], M. Villa[23a,23b], M. Villaplana Perez[162], E. M. Villhauer[52], E. Vilucchi[53], M. G. Vincter[34], G. S. Virdee[20], A. Vishwakarma[52], C. Vittori[23a,23b], I. Vivarelli[145], V. Vladimirov[166], E. Voevodina[109], F. Vogel[108], P. Vokac[131], J. Von Ahnen[48], E. Von Toerne[24], B. Vormwald[36], V. Vorobel[132], K. Vorobev[37], M. Vos[162], K. Voss[140], J. H. Vossebeld[91], M. Vozak[113], L. Vozdecky[93], N. Vranjes[15], M. Vranjes Milosavljevic[15], M. Vreeswijk[113], R. Vuillermet[36], O. Vujinovic[99], I. Vukotic[39], S. Wada[156], C. Wagner[102], W. Wagner[170], S. Wahdan[170], H. Wahlberg[89], R. Wakasa[156], M. Wakida[110], V. M. Walbrecht[109], J. Walder[133], R. Walker[108], W. Walkowiak[140], A. M. Wang[61], A. Z. Wang[169], C. Wang[62a], C. Wang[62c], H. Wang[17a], J. Wang[64a], R.-J. Wang[99], R. Wang[61], R. Wang[6], S. M. Wang[147], S. Wang[62b], T. Wang[62a], W. T. Wang[79], X. Wang[14c], X. Wang[161], X. Wang[62c], Y. Wang[62d], Y. Wang[14c], Z. Wang[105], Z. Wang[62d,51,62c], Z. Wang[105], A. Warburton[103], R. J. Ward[20], N. Warrack[59], A. T. Watson[20], H. Watson[59], M. F. Watson[20], G. Watts[137], B. M. Waugh[95], A. F. Webb[11], C. Weber[29], H. A. Weber[18], M. S. Weber[19], S. M. Weber[63a], C. Wei[62a], Y. Wei[125], A. R. Weidberg[125], J. Weingarten[49], M. Weirich[99], C. Weiser[54], C. J. Wells[48], T. Wenaus[29], B. Wendland[49], T. Wengler[36], N. S. Wenke[109], N. Wermes[24], M. Wessels[63a], K. Whalen[122], A. M. Wharton[90], A. S. White[61], A. White[8], M. J. White[1], D. Whiteson[159], L. Wickremasinghe[123], W. Wiedenmann[169], C. Wiel[50], M. Wielers[133], C. Wiglesworth[42], L. A. M. Wiik-Fuchs[54], D. J. Wilbern[119], H. G. Wilkens[36], D. M. Williams[41], H. H. Williams[127], S. Williams[32], S. Willocq[102], P. J. Windischhofer[125], F. Winklmeier[122], B. T. Winter[54], J. K. Winter[100], M. Wittgen[142], M. Wobisch[96], R. Wölker[125], J. Wollrath[159], M. W. Wolter[85], H. Wolters[129a,129c], V. W. S. Wong[163], A. F. Wongel[48], S. D. Worm[48], B. K. Wosiek[85], K. W. Woźniak[85], K. Wraight[59], J. Wu[14a,14d], M. Wu[64a], M. Wu[112], S. L. Wu[169], X. Wu[56], Y. Wu[62a], Z. Wu[134,62a], J. Wuerzinger[125], T. R. Wyatt[100], B. M. Wynne[52], S. Xella[42], L. Xia[14c], M. Xia[14b], J. Xiang[64c], X. Xiao[105], M. Xie[62a], X. Xie[62a], S. Xin[14a,14d], J. Xiong[17a], I. Xiotidis[145], D. Xu[14a], H. Xu[62a], H. Xu[62a], L. Xu[62a], R. Xu[127], T. Xu[105], W. Xu[105], Y. Xu[14b], Z. Xu[62b], Z. Xu[14a], B. Yabsley[146], S. Yacoob[33a], N. Yamaguchi[88], Y. Yamaguchi[153], H. Yamauchi[156], T. Yamazaki[17a], Y. Yamazaki[83], J. Yan[62c], S. Yan[125], Z. Yan[25], H. J. Yang[62c,62d], H. T. Yang[62a], S. Yang[62a], T. Yang[64c], X. Yang[62a], X. Yang[14a], Y. Yang[44], Z. Yang[62a,105], W-M. Yao[17a], Y. C. Yap[48], H. Ye[14c], H. Ye[55], J. Ye[44], S. Ye[29], X. Ye[62a], Y. Yeh[95], I. Yeletskikh[38], B. K. Yeo[17a], M. R. Yexley[90], P. Yin[41], K. Yorita[167], S. Younas[27b], C. J. S. Young[54], C. Young[142], M. Yuan[105], R. Yuan[62b,k], L. Yue[95], X. Yue[63a], M. Zaazoua[35e], B. Zabinski[85], E. Zaid[52], T. Zakareishvili[148b], N. Zakharchuk[34], S. Zambito[56], J. A. Zamora Saa[136b,136d], J. Zang[152], D. Zanzi[54], O. Zaplatilek[131], S. V. Zeißner[49], C. Zeitnitz[170], J. C. Zeng[161], D. T. Zenger Jr[26], O. Zenin[37], T. Ženiš[28a], S. Zenz[93], S. Zerradi[35a], D. Zerwas[66], M. Zhai[14a,14d], B. Zhang[14c], D. F. Zhang[138], J. Zhang[62b], J. Zhang[6], K. Zhang[14a,14d], L. Zhang[14c], P. Zhang[14a,14d], R. Zhang[169], S. Zhang[105], T. Zhang[152], X. Zhang[62c], X. Zhang[62b], Y. Zhang[62c,5], Z. Zhang[17a], Z. Zhang[66], H. Zhao[137], P. Zhao[51], T. Zhao[62b], Y. Zhao[135], Z. Zhao[62a], A. Zhemchugov[38], X. Zheng[62a], Z. Zheng[142], D. Zhong[161], B. Zhou[105], C. Zhou[169], H. Zhou[7], N. Zhou[62c], Y. Zhou[7], C. G. Zhu[62b], C. Zhu[14a,14d], H. L. Zhu[62a], H. Zhu[14a], J. Zhu[105], Y. Zhu[62c], Y. Zhu[62a], X. Zhuang[14a], K. Zhukov[37], V. Zhulanov[37], N. I. Zimine[38], J. Zinsser[63b], M. Ziolkowski[140], L. Živković[15], A. Zoccoli[23a,23b], K. Zoch[56], T. G. Zorbas[138], O. Zormpa[46], W. Zou[41], L. Zwalinski[36]

[1] Department of Physics, University of Adelaide, Adelaide, Australia
[2] Department of Physics, University of Alberta, Edmonton, AB, Canada
[3] [(a)]Department of Physics, Ankara University, Ankara, Türkiye; [(b)]Division of Physics, TOBB University of Economics and Technology, Ankara, Türkiye
[4] LAPP, Univ. Savoie Mont Blanc, CNRS/IN2P3, Annecy, France
[5] APC, Université Paris Cité, CNRS/IN2P3, Paris, France
[6] High Energy Physics Division, Argonne National Laboratory, Argonne, IL, USA
[7] Department of Physics, University of Arizona, Tucson, AZ, USA
[8] Department of Physics, University of Texas at Arlington, Arlington, TX, USA
[9] Physics Department, National and Kapodistrian University of Athens, Athens, Greece
[10] Physics Department, National Technical University of Athens, Zografou, Greece
[11] Department of Physics, University of Texas at Austin, Austin, TX, USA
[12] Institute of Physics, Azerbaijan Academy of Sciences, Baku, Azerbaijan
[13] Institut de Física d'Altes Energies (IFAE), Barcelona Institute of Science and Technology, Barcelona, Spain

[14] [(a)]Institute of High Energy Physics, Chinese Academy of Sciences, Beijing, China; [(b)]Physics Department, Tsinghua University, Beijing, China; [(c)]Department of Physics, Nanjing University, Nanjing, China; [(d)]University of Chinese Academy of Science (UCAS), Beijing, China
[15] Institute of Physics, University of Belgrade, Belgrade, Serbia
[16] Department for Physics and Technology, University of Bergen, Bergen, Norway
[17] [(a)]Physics Division, Lawrence Berkeley National Laboratory, Berkeley, CA, USA; [(b)]University of California, Berkeley, CA, USA
[18] Institut für Physik, Humboldt Universität zu Berlin, Berlin, Germany
[19] Albert Einstein Center for Fundamental Physics and Laboratory for High Energy Physics, University of Bern, Bern, Switzerland
[20] School of Physics and Astronomy, University of Birmingham, Birmingham, UK
[21] [(a)]Department of Physics, Bogazici University, Istanbul, Türkiye; [(b)]Department of Physics Engineering, Gaziantep University, Gaziantep, Türkiye; [(c)]Department of Physics, Istanbul University, Istanbul, Türkiye; [(d)]Istinye University, Sariyer, Istanbul, Türkiye
[22] [(a)]Facultad de Ciencias y Centro de Investigaciónes, Universidad Antonio Nariño, Bogotá, Colombia; [(b)]Departamento de Física, Universidad Nacional de Colombia, Bogotá, Colombia
[23] [(a)]Dipartimento di Fisica e Astronomia A. Righi, Università di Bologna, Bologna, Italy; [(b)]INFN Sezione di Bologna, Bologna, Italy
[24] Physikalisches Institut, Universität Bonn, Bonn, Germany
[25] Department of Physics, Boston University, Boston, MA, USA
[26] Department of Physics, Brandeis University, Waltham, MA, USA
[27] [(a)]Transilvania University of Brasov, Brasov, Romania; [(b)]Horia Hulubei National Institute of Physics and Nuclear Engineering, Bucharest, Romania; [(c)]Department of Physics, Alexandru Ioan Cuza University of Iasi, Iasi, Romania; [(d)]National Institute for Research and Development of Isotopic and Molecular Technologies, Physics Department, Cluj-Napoca, Romania; [(e)]University Politehnica Bucharest, Bucharest, Romania; [(f)]West University in Timisoara, Timisoara, Romania; [(g)]Faculty of Physics, University of Bucharest, Bucharest, Romania
[28] [(a)]Faculty of Mathematics, Physics and Informatics, Comenius University, Bratislava, Slovak Republic; [(b)]Department of Subnuclear Physics, Institute of Experimental Physics of the Slovak Academy of Sciences, Kosice, Slovak Republic
[29] Physics Department, Brookhaven National Laboratory, Upton, NY, USA
[30] Facultad de Ciencias Exactas y Naturales, Departamento de Física, y CONICET, Instituto de Física de Buenos Aires (IFIBA), Universidad de Buenos Aires, Buenos Aires, Argentina
[31] California State University, Fresno, CA, USA
[32] Cavendish Laboratory, University of Cambridge, Cambridge, UK
[33] [(a)]Department of Physics, University of Cape Town, Cape Town, South Africa; [(b)]iThemba Labs, Western Cape, South Africa; [(c)]Department of Mechanical Engineering Science, University of Johannesburg, Johannesburg, South Africa; [(d)]National Institute of Physics, University of the Philippines Diliman, Quezon City, Philippines; [(e)]Department of Physics, University of South Africa, Pretoria, South Africa; [(f)]University of Zululand, KwaDlangezwa, South Africa; [(g)]
School of Physics, University of the Witwatersrand, Johannesburg, South Africa
[34] Department of Physics, Carleton University, Ottawa, ON, Canada
[35] [(a)]Faculté des Sciences Ain Chock, Réseau Universitaire de Physique des Hautes Energies - Université Hassan II, Casablanca, Morocco; [(b)]Faculté des Sciences, Université Ibn-Tofail, Kénitra, Morocco; [(c)]Faculté des Sciences Semlalia, LPHEA-Marrakech, Université Cadi Ayyad, Marrakech, Morocco; [(d)]LPMR, Faculté des Sciences, Université Mohamed Premier, Oujda, Morocco; [(e)]Faculté des sciences, Université Mohammed V, Rabat, Morocco; [(f)]Institute of Applied Physics, Mohammed VI Polytechnic University, Ben Guerir, Morocco
[36] CERN, Geneva, Switzerland
[37] Affiliated with an Institute Covered by a Cooperation Agreement with CERN, Geneva, Switzerland
[38] Affiliated with an International Laboratory Covered by a Cooperation Agreement with CERN, Geneva, Switzerland
[39] Enrico Fermi Institute, University of Chicago, Chicago, IL, USA
[40] LPC, Université Clermont Auvergne, CNRS/IN2P3, Clermont-Ferrand, France
[41] Nevis Laboratory, Columbia University, Irvington, NY, USA
[42] Niels Bohr Institute, University of Copenhagen, Copenhagen, Denmark

[43] [(a)]Dipartimento di Fisica, Università della Calabria, Rende, Italy; [(b)]INFN Gruppo Collegato di Cosenza, Laboratori Nazionali di Frascati, Frascati, Italy
[44] Physics Department, Southern Methodist University, Dallas, TX, USA
[45] Physics Department, University of Texas at Dallas, Richardson, TX, USA
[46] National Centre for Scientific Research "Demokritos", Agia Paraskevi, Greece
[47] [(a)]Department of Physics, Stockholm University, Stockholm, Sweden; [(b)]Oskar Klein Centre, Stockholm, Sweden
[48] Deutsches Elektronen-Synchrotron DESY, Hamburg and Zeuthen, Germany
[49] Fakultät Physik , Technische Universität Dortmund, Dortmund, Germany
[50] Institut für Kern- und Teilchenphysik, Technische Universität Dresden, Dresden, Germany
[51] Department of Physics, Duke University, Durham, NC, USA
[52] SUPA-School of Physics and Astronomy, University of Edinburgh, Edinburgh, UK
[53] INFN e Laboratori Nazionali di Frascati, Frascati, Italy
[54] Physikalisches Institut, Albert-Ludwigs-Universität Freiburg, Freiburg, Germany
[55] II. Physikalisches Institut, Georg-August-Universität Göttingen, Göttingen, Germany
[56] Département de Physique Nucléaire et Corpusculaire, Université de Genève, Geneva, Switzerland
[57] [(a)]Dipartimento di Fisica, Università di Genova, Genoa, Italy; [(b)]INFN Sezione di Genova, Genoa, Italy
[58] II. Physikalisches Institut, Justus-Liebig-Universität Giessen, Giessen, Germany
[59] SUPA-School of Physics and Astronomy, University of Glasgow, Glasgow, UK
[60] LPSC, Université Grenoble Alpes, CNRS/IN2P3, Grenoble INP, Grenoble, France
[61] Laboratory for Particle Physics and Cosmology, Harvard University, Cambridge, MA, USA
[62] [(a)]Department of Modern Physics and State Key Laboratory of Particle Detection and Electronics, University of Science and Technology of China, Hefei, China; [(b)]Institute of Frontier and Interdisciplinary Science and Key Laboratory of Particle Physics and Particle Irradiation (MOE), Shandong University, Qingdao, China; [(c)]School of Physics and Astronomy, Key Laboratory for Particle Astrophysics and Cosmology (MOE), SKLPPC, Shanghai Jiao Tong University, Shanghai, China; [(d)]Tsung-Dao Lee Institute, Shanghai, China
[63] [(a)]Kirchhoff-Institut für Physik, Ruprecht-Karls-Universität Heidelberg, Heidelberg, Germany; [(b)]Physikalisches Institut, Ruprecht-Karls-Universität Heidelberg, Heidelberg, Germany
[64] [(a)]Department of Physics, Chinese University of Hong Kong, Shatin, N.T., Hong Kong, China; [(b)]Department of Physics, University of Hong Kong, Hong Kong, China; [(c)]Department of Physics and Institute for Advanced Study, Hong Kong University of Science and Technology, Clear Water Bay, Kowloon, Hong Kong, China
[65] Department of Physics, National Tsing Hua University, Hsinchu, Taiwan
[66] IJCLab, CNRS/IN2P3, Université Paris-Saclay, 91405 Orsay, France
[67] Department of Physics, Indiana University, Bloomington, IN, USA
[68] [(a)]INFN Gruppo Collegato di Udine, Sezione di Trieste, Udine, Italy; [(b)]ICTP, Trieste, Italy; [(c)]Dipartimento Politecnico di Ingegneria e Architettura, Università di Udine, Udine, Italy
[69] [(a)]INFN Sezione di Lecce, Lecce, Italy; [(b)]Dipartimento di Matematica e Fisica, Università del Salento, Lecce, Italy
[70] [(a)]INFN Sezione di Milano, Milan, Italy; [(b)]Dipartimento di Fisica, Università di Milano, Milan, Italy
[71] [(a)]INFN Sezione di Napoli, Naples, Italy; [(b)]Dipartimento di Fisica, Università di Napoli, Naples, Italy
[72] [(a)]INFN Sezione di Pavia, Pavia, Italy; [(b)]Dipartimento di Fisica, Università di Pavia, Pavia, Italy
[73] [(a)]INFN Sezione di Pisa, Pisa, Italy; [(b)]Dipartimento di Fisica E. Fermi, Università di Pisa, Pisa, Italy
[74] [(a)]INFN Sezione di Roma, Rome, Italy; [(b)]Dipartimento di Fisica, Sapienza Università di Roma, Rome, Italy
[75] [(a)]INFN Sezione di Roma Tor Vergata, Rome, Italy; [(b)]Dipartimento di Fisica, Università di Roma Tor Vergata, Rome, Italy
[76] [(a)]INFN Sezione di Roma Tre, Rome, Italy; [(b)]Dipartimento di Matematica e Fisica, Università Roma Tre, Rome, Italy
[77] [(a)]INFN-TIFPA, Trento, Italy; [(b)]Università degli Studi di Trento, Trento, Italy
[78] Universität Innsbruck, Department of Astro and Particle Physics, Innsbruck, Austria
[79] University of Iowa, Iowa City, IA, USA
[80] Department of Physics and Astronomy, Iowa State University, Ames, IA, USA
[81] [(a)]Departamento de Engenharia Elétrica, Universidade Federal de Juiz de Fora (UFJF), Juiz de Fora, Brazil; [(b)]Universidade Federal do Rio De Janeiro COPPE/EE/IF, Rio de Janeiro, Brazil; [(c)]Instituto de Física, Universidade de São Paulo, São Paulo, Brazil; [(d)]Rio de Janeiro State University, Rio de Janeiro, Brazil
[82] KEK, High Energy Accelerator Research Organization, Tsukuba, Japan
[83] Graduate School of Science, Kobe University, Kobe, Japan

[84] [(a)]AGH University of Science and Technology, Faculty of Physics and Applied Computer Science, Kraków, Poland; [(b)]Marian Smoluchowski Institute of Physics, Jagiellonian University, Kraków, Poland
[85] Institute of Nuclear Physics Polish Academy of Sciences, Kraków, Poland
[86] Faculty of Science, Kyoto University, Kyoto, Japan
[87] Kyoto University of Education, Kyoto, Japan
[88] Research Center for Advanced Particle Physics and Department of Physics, Kyushu University, Fukuoka , Japan
[89] Instituto de Física La Plata, Universidad Nacional de La Plata and CONICET, La Plata, Argentina
[90] Physics Department, Lancaster University, Lancaster, UK
[91] Oliver Lodge Laboratory, University of Liverpool, Liverpool, UK
[92] Department of Experimental Particle Physics, Jožef Stefan Institute and Department of Physics, University of Ljubljana, Ljubljana, Slovenia
[93] School of Physics and Astronomy, Queen Mary University of London, London, UK
[94] Department of Physics, Royal Holloway University of London, Egham, UK
[95] Department of Physics and Astronomy, University College London, London, UK
[96] Louisiana Tech University, Ruston, LA, USA
[97] Fysiska institutionen, Lunds universitet, Lund, Sweden
[98] Departamento de Física Teorica C-15 and CIAFF, Universidad Autónoma de Madrid, Madrid, Spain
[99] Institut für Physik, Universität Mainz, Mainz, Germany
[100] School of Physics and Astronomy, University of Manchester, Manchester, UK
[101] CPPM, Aix-Marseille Université, CNRS/IN2P3, Marseille, France
[102] Department of Physics, University of Massachusetts, Amherst, MA, USA
[103] Department of Physics, McGill University, Montreal, QC, Canada
[104] School of Physics, University of Melbourne, Victoria, Australia
[105] Department of Physics, University of Michigan, Ann Arbor, MI, USA
[106] Department of Physics and Astronomy, Michigan State University, East Lansing, MI, USA
[107] Group of Particle Physics, University of Montreal, Montreal, QC, Canada
[108] Fakultät für Physik, Ludwig-Maximilians-Universität München, Munich, Germany
[109] Max-Planck-Institut für Physik (Werner-Heisenberg-Institut), Munich, Germany
[110] Graduate School of Science and Kobayashi-Maskawa Institute, Nagoya University, Nagoya, Japan
[111] Department of Physics and Astronomy, University of New Mexico, Albuquerque, NM, USA
[112] Institute for Mathematics, Astrophysics and Particle Physics, Radboud University/Nikhef, Nijmegen, The Netherlands
[113] Nikhef National Institute for Subatomic Physics and University of Amsterdam, Amsterdam, The Netherlands
[114] Department of Physics, Northern Illinois University, DeKalb, IL, USA
[115] [(a)]New York University Abu Dhabi, Abu Dhabi, United Arab Emirates; [(b)]University of Sharjah, Sharjah, United Arab Emirates
[116] Department of Physics, New York University, New York, NY, USA
[117] Ochanomizu University, Otsuka, Bunkyo-ku, Tokyo, Japan
[118] Ohio State University, Columbus, OH, USA
[119] Homer L. Dodge Department of Physics and Astronomy, University of Oklahoma, Norman, OK, USA
[120] Department of Physics, Oklahoma State University, Stillwater, OK, USA
[121] Joint Laboratory of Optics, Palacký University, Olomouc, Czech Republic
[122] Institute for Fundamental Science, University of Oregon, Eugene, OR, USA
[123] Graduate School of Science, Osaka University, Osaka, Japan
[124] Department of Physics, University of Oslo, Oslo, Norway
[125] Department of Physics, Oxford University, Oxford, UK
[126] LPNHE, Sorbonne Université, Université Paris Cité, CNRS/IN2P3, Paris, France
[127] Department of Physics, University of Pennsylvania, Philadelphia, PA, USA
[128] Department of Physics and Astronomy, University of Pittsburgh, Pittsburgh, PA, USA
[129] [(a)]Laboratório de Instrumentação e Física Experimental de Partículas - LIP, Lisbon, Portugal; [(b)]Departamento de Física, Faculdade de Ciências, Universidade de Lisboa, Lisbon, Portugal; [(c)]Departamento de Física, Universidade de Coimbra, Coimbra, Portugal; [(d)]Centro de Física Nuclear da Universidade de Lisboa, Lisbon, Portugal; [(e)]Departamento de Física, Universidade do Minho, Braga, Portugal; [(f)]Departamento de Física Teórica y del Cosmos, Universidad de Granada,

Granada (Spain), Portugal; [g]Departamento de Física, Instituto Superior Técnico, Universidade de Lisboa, Lisbon, Portugal
[130] Institute of Physics of the Czech Academy of Sciences, Prague, Czech Republic
[131] Czech Technical University in Prague, Prague, Czech Republic
[132] Faculty of Mathematics and Physics, Charles University, Prague, Czech Republic
[133] Particle Physics Department, Rutherford Appleton Laboratory, Didcot, UK
[134] IRFU, CEA, Université Paris-Saclay, Gif-sur-Yvette, France
[135] Santa Cruz Institute for Particle Physics, University of California Santa Cruz, Santa Cruz, CA, USA
[136] [a]Departamento de Física, Pontificia Universidad Católica de Chile, Santiago, Chile; [b]Millennium Institute for Subatomic physics at high energy frontier (SAPHIR), Santiago, Chile; [c]Instituto de Investigación Multidisciplinario en Ciencia y Tecnología, y Departamento de Física, Universidad de La Serena, La Serena, Chile; [d]Universidad Andres Bello, Department of Physics, Santiago, Chile; [e]Instituto de Alta Investigación, Universidad de Tarapacá, Arica, Chile; [f]Departamento de Física, Universidad Técnica Federico Santa María, Valparaiso, Chile
[137] Department of Physics, University of Washington, Seattle, WA, USA
[138] Department of Physics and Astronomy, University of Sheffield, Sheffield, UK
[139] Department of Physics, Shinshu University, Nagano, Japan
[140] Department Physik, Universität Siegen, Siegen, Germany
[141] Department of Physics, Simon Fraser University, Burnaby, BC, Canada
[142] SLAC National Accelerator Laboratory, Stanford, CA, USA
[143] Department of Physics, Royal Institute of Technology, Stockholm, Sweden
[144] Departments of Physics and Astronomy, Stony Brook University, Stony Brook, NY, USA
[145] Department of Physics and Astronomy, University of Sussex, Brighton, UK
[146] School of Physics, University of Sydney, Sydney, Australia
[147] Institute of Physics, Academia Sinica, Taipei, Taiwan
[148] [a]E. Andronikashvili Institute of Physics, Iv. Javakhishvili Tbilisi State University, Tbilisi, Georgia; [b]High Energy Physics Institute, Tbilisi State University, Tbilisi, Georgia; [c]University of Georgia, Tbilisi, Georgia
[149] Department of Physics, Technion, Israel Institute of Technology, Haifa, Israel
[150] Raymond and Beverly Sackler School of Physics and Astronomy, Tel Aviv University, Tel Aviv, Israel
[151] Department of Physics, Aristotle University of Thessaloniki, Thessaloníki, Greece
[152] International Center for Elementary Particle Physics and Department of Physics, University of Tokyo, Tokyo, Japan
[153] Department of Physics, Tokyo Institute of Technology, Tokyo, Japan
[154] Department of Physics, University of Toronto, Toronto, ON, Canada
[155] [a]TRIUMF, Vancouver, BC, Canada; [b]Department of Physics and Astronomy, York University, Toronto, ON, Canada
[156] Division of Physics and Tomonaga Center for the History of the Universe, Faculty of Pure and Applied Sciences, University of Tsukuba, Tsukuba, Japan
[157] Department of Physics and Astronomy, Tufts University, Medford, MA, USA
[158] United Arab Emirates University, Al Ain, United Arab Emirates
[159] Department of Physics and Astronomy, University of California Irvine, Irvine, CA, USA
[160] Department of Physics and Astronomy, University of Uppsala, Uppsala, Sweden
[161] Department of Physics, University of Illinois, Urbana, IL, USA
[162] Instituto de Física Corpuscular (IFIC), Centro Mixto Universidad de Valencia-CSIC, Valencia, Spain
[163] Department of Physics, University of British Columbia, Vancouver, BC, Canada
[164] Department of Physics and Astronomy, University of Victoria, Victoria, BC, Canada
[165] Fakultät für Physik und Astronomie, Julius-Maximilians-Universität Würzburg, Würzburg, Germany
[166] Department of Physics, University of Warwick, Coventry, UK
[167] Waseda University, Tokyo, Japan
[168] Department of Particle Physics and Astrophysics, Weizmann Institute of Science, Rehovot, Israel
[169] Department of Physics, University of Wisconsin, Madison, WI, USA
[170] Fakultät für Mathematik und Naturwissenschaften, Fachgruppe Physik, Bergische Universität Wuppertal, Wuppertal, Germany
[171] Department of Physics, Yale University, New Haven, CT, USA

[a] Also at Also Affiliated with an Institute Covered by a Cooperation Agreement with CERN, Geneva, Switzerland
[b] Also at Borough of Manhattan Community College, City University of New York, New York, NY, USA
[c] Also at Bruno Kessler Foundation, Trento, Italy
[d] Also at Center for High Energy Physics, Peking University, Beijing, China
[e] Also at Center for Interdisciplinary Research and Innovation (CIRI-AUTH), Thessaloníki, Greece
[f] Also at Centro Studi e Ricerche Enrico Fermi, Rome, Italy
[g] Also at CERN, Geneva, Switzerland
[h] Also at Département de Physique Nucléaire et Corpusculaire, Université de Genève, Geneva, Switzerland
[i] Also at Departament de Fisica de la Universitat Autonoma de Barcelona, Barcelona, Spain
[j] Also at Department of Financial and Management Engineering, University of the Aegean, Chios, Greece
[k] Also at Department of Physics and Astronomy, Michigan State University, East Lansing, MI, USA
[l] Also at Department of Physics and Astronomy, University of Louisville, Louisville, KY, USA
[m] Also at Department of Physics, Ben Gurion University of the Negev, Beer Sheva, Israel
[n] Also at Department of Physics, California State University, East Bay, USA
[o] Also at Department of Physics, California State University, Sacramento, USA
[p] Also at Department of Physics, King's College London, London, UK
[q] Also at Department of Physics, University of Fribourg, Fribourg, Switzerland
[r] Also at Department of Physics, University of Thessaly, Volos, Greece
[s] Also at Department of Physics, Westmont College, Santa Barbara, USA
[t] Also at Hellenic Open University, Patras, Greece
[u] Also at Institucio Catalana de Recerca i Estudis Avancats, ICREA, Barcelona, Spain
[v] Also at Institut für Experimentalphysik, Universität Hamburg, Hamburg, Germany
[w] Also at Institute of Applied Physics, Mohammed VI Polytechnic University, Ben Guerir, Morocco
[x] Also at Institute of Particle Physics (IPP), Toronto, Canada
[y] Also at Institute of Physics and Technology, Ulaanbaatar, Mongolia
[z] Also at Institute of Physics, Azerbaijan Academy of Sciences, Baku, Azerbaijan
[aa] Also at Institute of Theoretical Physics, Ilia State University, Tbilisi, Georgia
[ab] Also at Lawrence Livermore National Laboratory, Livermore, USA
[ac] Also at RWTH Aachen University, III. Physikalisches Institut A, Aachen, Germany
[ad] Also at The Collaborative Innovation Center of Quantum Matter (CICQM), Beijing, China
[ae] Also at TRIUMF, Vancouver, BC, Canada
[af] Also at Università di Napoli Parthenope, Naples, Italy
[ag] Also at University of Chinese Academy of Sciences (UCAS), Beijing, China
[ah] Also at Department of Physics, University of Colorado Boulder, Colorado, USA
[ai] Also at Washington College, Maryland, USA
[aj] Also at Physics Department, Yeditepe University, Istanbul, Türkiye
[ak] Also at Physics Department, An-Najah National University, Nablus, Palestine
[al] Also at University of Colorado Boulder, Department of Physics, Colorado, USA
[am] Also at L2IT, Université de Toulouse, CNRS/IN2P3, UPS, Toulouse, France
[an] Also at Technical University of Munich, Munich, Germany
[ao] Also at Department of Physics, Stanford University, Stanford, CA, USA
[ap] Also at Institute for Nuclear Research and Nuclear Energy (INRNE) of the Bulgarian Academy of Sciences, Sofia, Bulgaria
* Deceased